

Review

Progress to Clarify How *NOTCH3* Mutations Lead to CADASIL, a Hereditary Cerebral Small Vessel Disease

Ikuko Mizuta ¹, Yumiko Nakao-Azuma ^{1,2}, Hideki Yoshida ³, Masamitsu Yamaguchi ^{3,4}
and Toshiki Mizuno ^{1,*}

¹ Department of Neurology, Graduate School of Medical Science, Kyoto Prefectural University of Medicine, 465 Kajji-cho, Kamigyo-ku, Kyoto 602-8566, Japan; imizuta@koto.kpu-m.ac.jp (I.M.)

² Department of Rehabilitation Medicine, Gunma University Graduate School of Medicine, Showa-machi, Maebashi, Gunma 371-8511, Japan

³ Department of Applied Biology, Kyoto Institute of Technology, Matsugasaki, Sakyo-ku, Kyoto 606-8585, Japan

⁴ Kansai Gakken Laboratory, Kankyo Eisei Yakuhin Co., Ltd., 3-6-2 Hikaridai, Seika-cho, Kyoto 619-0237, Japan

* Correspondence: mizuno@koto.kpu-m.ac.jp; Tel.: +81-75-251-5793

Abstract: Notch signaling is conserved in *C. elegans*, *Drosophila*, and mammals. Among the four *NOTCH* genes in humans, *NOTCH1*, *NOTCH2*, and *NOTCH3* are known to cause monogenic hereditary disorders. Most *NOTCH*-related disorders are congenital and caused by a gain or loss of Notch signaling activity. In contrast, cerebral autosomal dominant arteriopathy with subcortical infarcts and leukoencephalopathy (CADASIL) caused by *NOTCH3* is adult-onset and considered to be caused by accumulation of the mutant *NOTCH3* extracellular domain (N3ECD) and, possibly, by an impairment in Notch signaling. Pathophysiological processes following mutant N3ECD accumulation have been intensively investigated; however, the process leading to N3ECD accumulation and its association with canonical *NOTCH3* signaling remain unknown. We reviewed the progress in clarifying the pathophysiological process involving mutant *NOTCH3*.

Keywords: Notch signaling; CADASIL; *NOTCH3*; EGF-like repeat; extracellular domain; granular osmiophilic material (GOM); transendocytosis; extracellular matrix protein



Citation: Mizuta, I.; Nakao-Azuma, Y.; Yoshida, H.; Yamaguchi, M.; Mizuno, T. Progress to Clarify How *NOTCH3* Mutations Lead to CADASIL, a Hereditary Cerebral Small Vessel Disease. *Biomolecules* **2024**, *14*, 127. <https://doi.org/10.3390/biom14010127>

Academic Editor: Martin Baron

Received: 8 December 2023

Revised: 9 January 2024

Accepted: 16 January 2024

Published: 18 January 2024



Copyright: © 2024 by the authors. Licensee MDPI, Basel, Switzerland. This article is an open access article distributed under the terms and conditions of the Creative Commons Attribution (CC BY) license (<https://creativecommons.org/licenses/by/4.0/>).

1. Introduction

Cerebral autosomal dominant arteriopathy with subcortical infarcts and leukoencephalopathy (CADASIL) is the most common form of hereditary cerebral small vessel disease and is characterized by recurrent stroke events, mood disturbance, and cognitive impairment [1]. The causative gene *NOTCH3* encodes the *NOTCH3* receptor protein, which mediates Notch signaling. All known causative mutations of CADASIL are located in the *NOTCH3* epidermal growth factor-like repeat (EGFr) domain, which is part of the *NOTCH3* extracellular domain (N3ECD). Most of the mutations are cysteine-altering missense mutations, resulting in alterations in the number of cysteine residues in a certain EGFr to an odd number [2]. Notch signaling is conserved from *C. elegans* to humans, and some *Drosophila melanogaster Notch (N)* lines harbor cysteine-altering mutations in the EGFr domain, corresponding to CADASIL-causing mutations. However, animal models of CADASIL other than rodent models have not been established. This may be partly because Notch signaling is not impaired in the presence of most CADASIL-causing mutations. Many in vitro and in vivo studies have suggested that accumulation of mutant N3ECD leads to CADASIL [3]; however, the precise mechanism of N3ECD accumulation and its association with Notch signaling remain unknown. In this review, we introduce animal and cellular models of CADASIL to discuss the pathophysiology of CADASIL-causing *NOTCH3* mutations.

2. Overview of CADASIL

2.1. Cerebral Small Vessel Diseases

Cerebrovascular disease, that is, brain circulation disorder, is manifested by stroke and transient ischemic attack (TIA). Stroke is an acute neurologic injury due to brain ischemia (~80%) or brain hemorrhage (~20%) [4], which can be diagnosed by neurological examination and neuroimaging, computed tomography (CT), and/or magnetic resonance imaging (MRI). Ischemic brain injury, called infarction, is permanent. TIA is now defined as a transient episode of neurologic dysfunction caused by focal brain, spinal cord, or retinal ischemia, without acute infarction [5].

Lesions of not only large but also small vessels predispose humans to brain ischemia (Figure 1). From clinical and pathological perspectives, small vessels in the brain generally correspond to small arteries or arterioles perforating brain parenchyma. Clinical and neuroimaging characteristics of cerebral small vessel disease are small lacunar infarcts (small ischemic lesions), microbleeds, white matter lesions, and vascular dementia [6]. Most patients are sporadic, with onsets and progressions being age-dependent and lifestyle-related. Patients suffer from stroke at 65 years old (y.o.) or older and have certain conventional cardiovascular risk factors, including hypertension, dyslipidemia, diabetes, arrhythmia, and smoking [6].

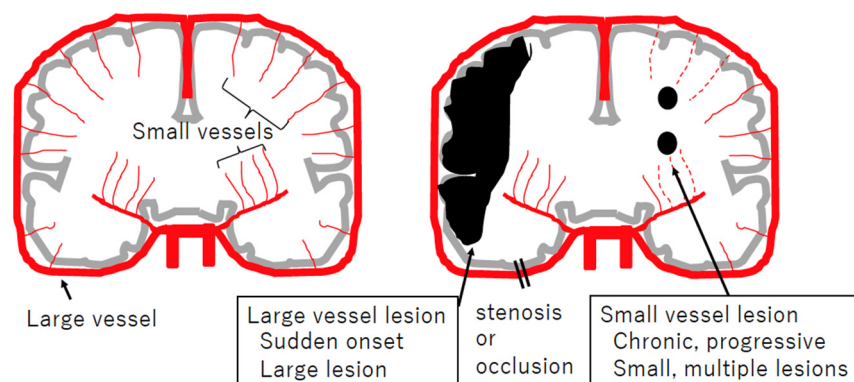


Figure 1. Schematic view of large and small vessel diseases, focusing on cerebral infarction. Coronary sections of the brain (gray), arteries (red), and ischemic lesions (black) are illustrated. Large artery obstruction usually occurs suddenly and results in ischemia in that region. Dysfunction of small arteries is usually chronic and progressive, resulting in small and multiple lesions, referred to as lacunar infarctions.

In contrast, rare hereditary, monogenic small vessel diseases are typically characterized by young onset and recurrent stroke episodes without cardiovascular risk factors. To date, around eight causative genes have been identified in hereditary small vessel diseases [7], and CADASIL is the most common form worldwide, with an estimated prevalence of 2–5/100,000 [8].

2.2. History of Disease Concept of CADASIL

Since 1955, independent families with hereditary cerebral small vessel diseases have been reported mainly from Europe. Retrospectively, the first patient with CADASIL was identified in 1976 [1,2]. In 1993, the acronym CADASIL was proposed to designate the autosomal dominant form of cerebral small vessel disease mapped to chromosome 19 [9]. Pathological examination of autopsied brains of CADASIL patients revealed the deposition of granular material in the media of small arteries [10,11]. The deposit was generically named granular osmiophilic material (GOM) in 1995 [12] and identified as a pathological hallmark of CADASIL [13]. GOM can be detected by electron microscopic observation of areas within or adjacent to the basement membrane of vascular smooth muscle cells (VSMCs) of systemic arterioles (Figure 2); therefore, skin biopsy is useful for the definitive diagnosis of CADASIL [12].

Linkage analysis finally determined the CADASIL locus as chromosome 19p13 [14,15]. In 1996, through cDNA library screening involving the CADASIL locus, Joutel et al. characterized the *NOTCH3* gene, the human homologue of mouse *Notch3*, and identified *NOTCH3* mutations in patients [15]. As a result, CADASIL can now be definitively diagnosed through genetic testing of *NOTCH3* or detection of GOM in skin biopsy specimens, consistent with the first guideline on the diagnosis and management of cerebral small vessel diseases recently proposed by the European Academy of Neurology [16].

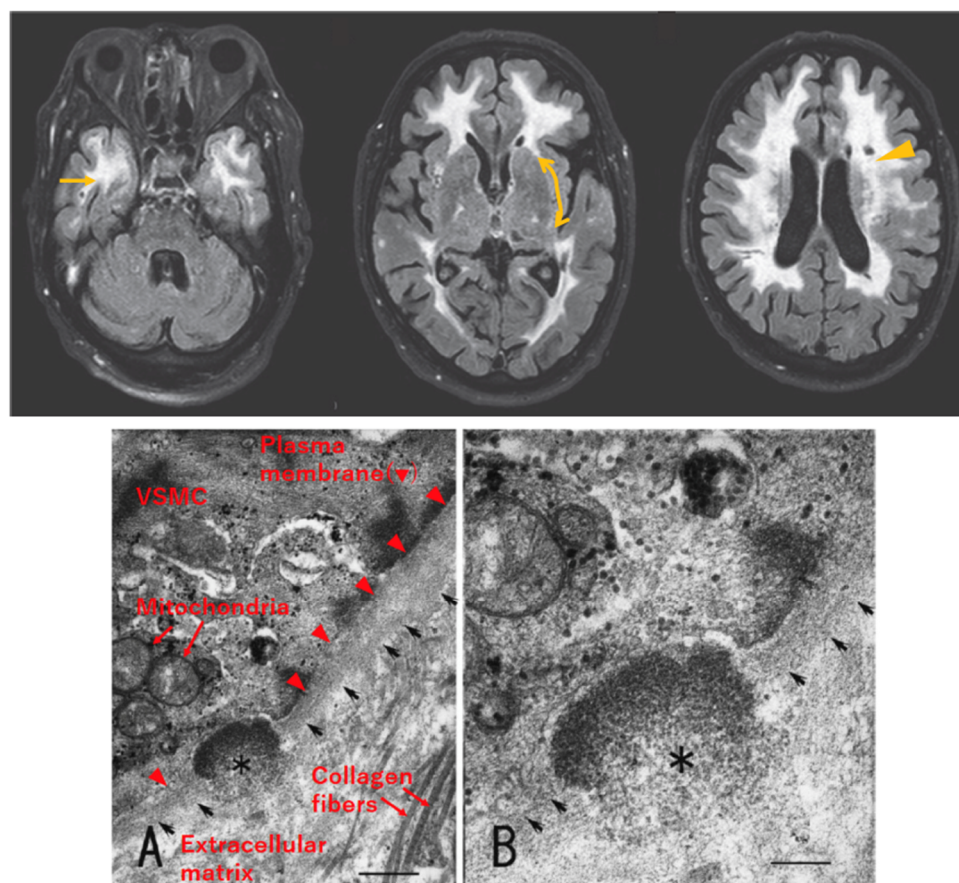


Figure 2. Radiological and pathological characteristics of CADASIL. Upper: Axial section of fluid-attenuated inversion recovery (FLAIR) MRI of a patient with CADASIL, reproduced with permission from Mizuno, 2012 [17], published by the Japanese Society of Neurology, with slight modification. White matter lesions are detected as hyperintense areas in deep white matter, including the temporal pole (left, arrow) and external capsule (middle, bidirectional arrow, faint signal in this patient). Lacunar infarcts are detected as punctiform low-intensity lesions (right, arrowhead). Lower: Electron micrograph of skin biopsy specimen, reproduced with permission from Mizuno et al., 2008 [18], published by the Japanese Society of Internal Medicine, with slight modification. Granular osmiophilic material (GOM, asterisk) exists within the basement membrane (arrows) of vascular smooth muscle cells (VSMCs). Labeling of cellular structures is presented in red in (A). Scale bar indicates 410 nm in (A) and 200 nm in (B).

2.3. Clinical Characteristics of CADASIL

The typical natural history of CADASIL was concisely described in previous reviews [1,2,19]. Briefly, as the disease progresses, migraine with aura, stroke/TIA, mood disturbance, apathy, motor disability, and dementia occur sequentially in this order. Migraine often occurs as the initial symptom, at 6–48 (mean: 30) y.o. [2]. Although most patients have few or no vascular risk factors, including hypertension, hyperlipidemia, diabetes, and smoking, they suffer from stroke/TIA repeatedly. The mean age at onset

of the initial ischemic event is around 49 y.o. [2], which is younger compared with that in sporadic stroke patients [20]. Neurological symptoms include motor palsy, pseudo-bulbar palsy, sensory disturbance, parkinsonism, and seizure. Additional symptoms are psychiatric disturbances, including severe mood disturbance (20% of patients) and apathy (40% of symptomatic patients) [2]. Executive dysfunction is detected by neuropsychological tests in 89% of patients, even in the early stages of the disease [21]. Cognitive impairment progresses, and dementia is present in 90% of patients prior to death [1].

White matter lesions (WMLs) are present as symmetrical hyperintense signals on T2-weighted or fluid-attenuated inversion recovery (FLAIR) MRI (Figure 2) in the early stages of the disease, preceding ischemic events [2]. WMLs often involve the periventricular region, external capsule, and/or temporal pole, and the lesion volume increases with aging. Especially, WMLs in the temporal pole show high sensitivity (90%) and high specificity (90%) for the diagnosis of CADASIL [19]. Regarding WMLs in the external capsule, their sensitivity for the diagnosis of CADASIL is also high, at 90%; however, their specificity is low, at 50% [19]. Other findings related to small vessel disease, lacunar infarcts and microbleeds, can also be detected in CADASIL patients [2].

It was reported that WMLs were detected in a 21 y.o. individual, who was an asymptomatic member of a CADASIL family [22]. In addition, it was reported that GOM was detected in a 19 y.o. patient, although it was not stated whether he/she was symptomatic [23]. These findings suggest that the imaging and pathological characteristics of CADASIL can be detected as early as around 20 y.o., being earlier than clinical symptoms.

2.4. Pathology of CADASIL

Histopathological findings in CADASIL patients include the thickening of vascular walls, luminal stenosis, and degeneration of VSMCs and pericytes, resembling those of sporadic small vessel diseases [13,24,25]. As described above, a CADASIL-specific pathological finding is GOM deposition within or adjacent to the basement membrane of VSMCs or pericytes detected on electron microscopic observation (Figure 2). GOM deposits often localize in infoldings of VSMCs and in close contact with the plasma membrane but separated from the plasma membrane by a thin electron-lucent halo; however, they are sometimes observed distant from the plasma membrane [26–28]. NOTCH3 consists of an extracellular domain (N3ECD) and intracellular domain (N3ICD) (see Section 3.1). Using antibodies against N3ECD or N3ICD, light and electron microscopic observations showed that N3ECD, not N3ICD, is accumulated in vessel walls and colocalized with GOM deposits [26,28,29].

2.5. Genetics of CADASIL

2.5.1. Autosomal Dominant Inheritance

CADASIL is inherited in an autosomal dominant manner, and most patients have heterozygous mutations. Patients with homozygous mutations have also been reported. Although some of them showed a more severe phenotype than heterozygous patients in the same family, the range of phenotypic severity in homozygous patients is considered to be similar to that in heterozygous patients [30].

2.5.2. Typical Cysteine-Altering Mutations in EGFr of NOTCH3

The *NOTCH3* gene spans 42 kb and consists of 33 exons. Nearly 300 *NOTCH3* mutations related to CADASIL have been reported [21,31–33]. All known mutations are located in the NOTCH3 EGFr domain (see Section 3.1), encoded by exons 2–24. Each EGFr normally contains six cysteine residues that are considered to form three pairs of disulfide bonds to stabilize the protein conformation and possibly form disulfide bonds with cysteines from the neighboring repeat domain. Most pathogenic mutations are cysteine-altering missense ones, resulting in a change in the number of cysteine residues in a certain EGFr to an odd number, disrupting the structure of not only the repeat the variant is within but also the neighboring repeat domain. Consequently, protein misfolding and/or interaction with

another molecule via an unpaired cysteine can occur [34,35], which may lead to the formation of GOM deposits. The extracellular accumulation of misfolded N3ECD may be due to exocytosis, aggregation on the plasma membrane, and/or impairment of transendocytosis (see Section 5.2.2), although the precise mechanism remains unknown.

2.5.3. Atypical Mutations in NOTCH3

A few cysteine-sparing mutations in *NOTCH3* were reported in CADASIL patients [36]. Among them, the substitution of arginine at amino acid position 75 of NOTCH3 to proline (p.Arg75Pro) is relatively common in Japanese and Korean patients with CADASIL [37–39], with convincing evidence of pathogenicity based on a segregation study and detection of GOM by skin biopsy [18]. Patients with p.Arg75Pro showed a lower frequency of temporal pole WML and later onset compared with patients with cysteine-altering mutations, suggesting an association of p.Arg75Pro with atypical and mild phenotypes [38–40].

p.Arg544Cys is a cysteine-altering mutation, pathologically confirmed by detecting GOM [41], but it is atypical because it localizes not in EGFr but between EGFr 13 and 14. Patients with p.Arg544Cys are frequently identified on Jeju Island in Korea and in Taiwan. Totals of 90.3 and 70.5% of CADASIL patients on Jeju Island and in Taiwan, respectively, were reported to have p.Arg544Cys [42,43]. In addition, patients with homozygous p.Arg544Cys have been repeatedly reported [41]. p.Arg544Cys is correlated with a low frequency of WMLs in the temporal pole and late age at onset [43], similar to p.Arg75Pro.

2.5.4. EGFr Location–Phenotype Correlations

As for typical cysteine-altering mutations, some genotype–phenotype correlation studies have been reported [39,44]. However, because of numerous mutations and various genotype distributions among populations, replication studies are considered difficult. Recently, the effect of the location of cysteine-altering mutations on the CADASIL phenotype has been suggested [45]. In CADASIL patients, typical cysteine-altering mutations are mostly located in EGFr 1–6 among the 34 EGFr [8]. In contrast, cysteine-altering *NOTCH3* variants in a general population, revealed by recent large-scale genetic variation databases, accumulated in EGFr 7–34 [8]. Total frequencies of variants of the general population were 0.4–11.7/1000, being approximately 100-fold higher than the prevalence of CADASIL, at 2–5/100,000, suggesting that *NOTCH3* variant carriers in general populations may be asymptomatic or preclinical CADASIL patients, or the variant may be of low penetrance [8]. Based on the difference in the variation hotspot between CADASIL patients and general individuals, Rutten et al. compared the disease severity between patients with EGFr 1–6 mutations and those with EGF 7–34 ones. They found that cysteine-altering mutations in EGFr 1–6 were associated with a more severe phenotype, earlier age at onset of stroke, and shorter life expectancy, than those in EGFr 7–34 [45]. An earlier age at onset of stroke in EGFr 1–6 was also noted in a Japanese study, suggesting that the effect of the mutation location on the phenotype is a consensus finding in CADASIL worldwide.

Recently, Hack et al. suggested a three-tiered EGFr domain stratification, high risk (EGFr 1–6, 8, 11, and 26), medium risk (EGFr 9–10, 12–15, 17, 25, 27, and 32), and low risk (EGFr 16, 18–20, 23–24, 28–31, and 33), according to intensive analysis of the literature on CADASIL and population genome databases [46]. A comparison of MRI findings, stroke risks, and pathological findings among these groups supported this classification [46].

3. NOTCH3 and Notch Signaling

3.1. Protein Structure of NOTCH3 Receptor

Notch family members and their ligands are single-pass transmembrane proteins. Notch is encoded by a single gene, *Notch* (*N*), in *Drosophila*, whereas there are four *Notch* family genes, *NOTCH1–4*, in mammals. The predominant form of cell surface Notch protein is a heterodimer of NECD and Notch intracellular domain (NICD) in both *Drosophila* and mammals [47]. NOTCH3, as well as other NOTCH family proteins, is S1-cleaved in the trans-Golgi network and then produces a non-covalent heterodimer of N3ECD

and N3ICD [48]. The molecular sizes of full-length NOTCH3, N3ECD, and N3ICD are 290, 230, and 95 kDa, respectively [49]. N3ECD includes 34 EGFr and Lin12-Notch repeats (LNRs). N3ICD contains the transmembrane domain (TMD), RBP η k association module (RAM), nuclear localization sequences (NLSs), ankyrin repeats (ANK), and proline/glutamate/serine/threonine motifs (PEST) (Figure 3) [48,50]. Mammalian Notch ligands are Jagged-1,2 (Jag1, Jag2) and Delta-like-1, 3, 4 (Dll1, Dll3, Dll4), which correspond to fly Serrate and Delta, respectively. Ligand–receptor interaction is mediated by the DSL (Delta, Serrate, LAG-2) domain of the ligand and EGFr domain of the receptor. *Drosophila* Notch contains 36 EGFr. An aggregation assay using *Drosophila* S2 cells transfected with deletion constructs of *Notch* and those transfected with *Serrate/Delta* showed that EGFr 11–12 of fly Notch were sufficient and necessary for ligand binding [51]. Through sequence comparison, EGFr 10–11 of human NOTCH3, corresponding to fly Notch EGFr 11–12, were predicted to mediate ligand binding [52], which was supported by a Notch signaling activity assay using human 293T cells transfected with the NOTCH3 construct lacking EGFr 10–11 [53].

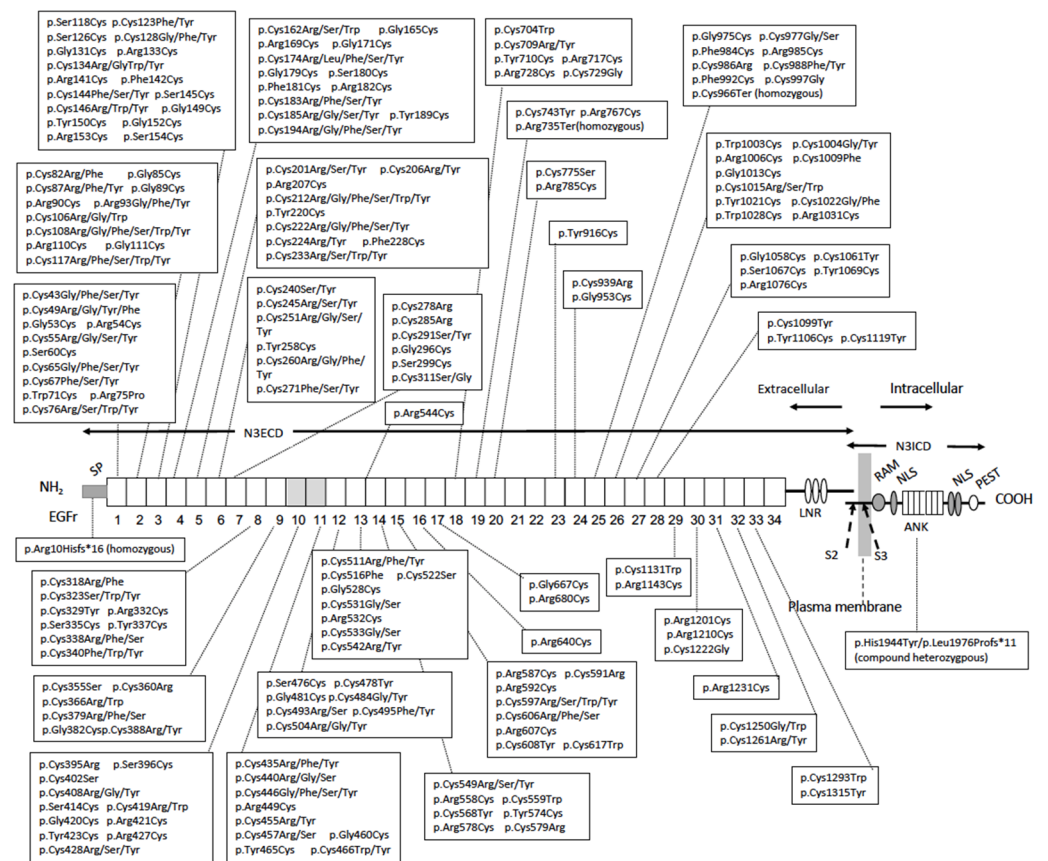


Figure 3. Structure of NOTCH3 receptor protein. NOTCH3 receptor is a non-covalent heterodimer of the extracellular domain (N3ECD) and intracellular domain (N3ICD). N3ECD contains the signal peptide (SP), 34 epidermal growth factor-like repeats (EGFr), of which the 10–11th ones are the ligand binding domain (shaded) and Lin-12/Notch repeat (LNR). N3ICD contains the RBP η k association module (RAM), ankyrin repeat (ANK), and nuclear localizing sequence (NLS), and is rich in proline (P), glutamate (E), serine (S), and threonine (T) (PEST) domains. The S2 cleavage site (S2) by “a disintegrin and metalloproteinases” (ADAM) protease and intramembrane S3 cleavage site (S3) by γ -secretase are shown. NOTCH3 mutations reported in CADASIL (Section 2.5 and HGMD Professional 2023.3 [54]) and bi-allelic loss-of-function mutations reported in autosomal recessive early-onset arteriopathy (see Section 5.1) [55–57] and their localizations are shown.

3.2. Notch Signaling Process

The Notch signaling process is complex (Figure 4). In the heterodimeric Notch receptor, the membrane-tethered NICD is kept inactivated by LNR of the Notch extracellular domain (NECD). Following ligand–receptor binding, via DSL of the ligand and EGFr of NECD, NECD is detached from NICD to be transendocytosed to a ligand-presenting cell [58]. The remaining NICD is activated by a sequential S2- and S3- proteolytic process. The membrane-bound “a disintegrin and metalloproteinases” (ADAM) proteases, mainly ADAM10 and ADAM17, participate in juxtamembrane S2-cleavage of NICD. Then, intramembrane S3-cleavage by γ -secretase occurs to allow NICD to leave the membrane. In the nucleus, the transcription regulator RBPjk associates with the co-repressor and represses promoter activity. After S3-cleaved NICD enters the nucleus via NLS, NICD interacts with RBPjk via the RBPjk association module (RAM) and ankyrin repeat (ANK), and then the co-repressor is swapped with the co-activator, resulting in activation of transcription of the target genes, including HES1 and HEYL [48,59].

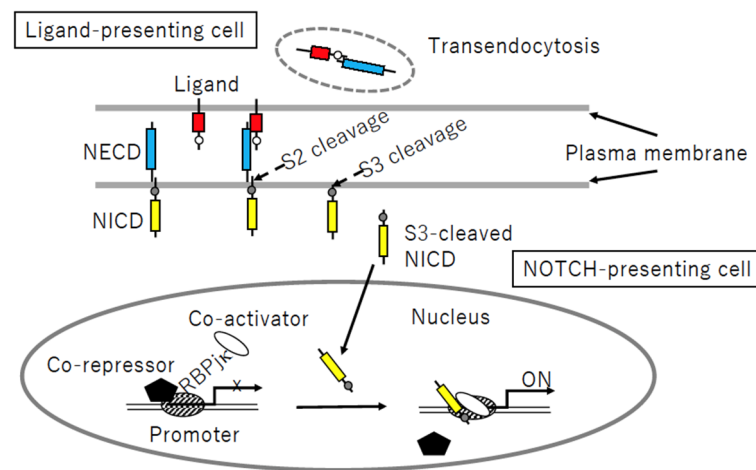


Figure 4. Notch signaling process. Following receptor–ligand binding, sequential S2- and S3-cleavage of the Notch intracellular domain (NICD, yellow) allows the cleaved protein to enter the nucleus, whereas the (red) ligand–Notch extracellular domain (NECD, blue) complex is transendocytosed into a ligand-presenting cell. Nuclear NICD is associated with the DNA-binding protein RBPjk, followed by detachment of the co-repressor and recruitment of the co-activator, resulting in target gene activation.

3.3. Localization of NOTCH Family Members and Their Ligands in Vessels

An immunohistochemical study of an autopsied specimen showed that NOTCH3 was expressed in VSMCs but not detected in endothelial cells [26]. The expression profiles of Notch family members and their ligands in blood vessel cells have been intensively analyzed in the mouse embryo, pre- and post-natal mouse brain [60], and retina [61]. Hofmann and Iruela-Arispe summarized the expression profiles as follows: Notch1, Notch3, Jag1, Jag2, and Dll1 are expressed in VSMCs, whereas Notch1, Notch4, Dll1, Dll4, and Jag1 are expressed in endothelial cells [62]. The NOTCH3-JAG1 interaction is focused on in CADASIL research, because Jagged1 is expressed in both endothelial cells and VSMCs, and the co-expression of JAG1 and NOTCH3 was detected in adult humans [53]. Notch signaling in the crosstalk between VSMCs and endothelial cells is considered to play an important role in VSMC maturation [63]. Endothelial or VSMC-specific deletion in mice strongly suggests that NOTCH3-JAG1 interaction occurs between endothelial cells and VSMCs and also between neighboring VSMCs. Mice with endothelial-specific deletion of Jag1 are embryonic-lethal, showing markedly decreased expression levels of VSMC markers but intact expression levels of endothelial markers [64]. Tamoxifen-induced conditional knockout of endothelial Jag1 in adult mice caused a loss of Jag1 expression and also decreased expressions of Notch3 and its downstream molecules in neighboring VSMCs [65].

Similarly, mice with VSMC-specific deletion of Jag1 are perinatal-lethal, showing a deficit in VSMC development [66], and the conditional knockout of VSMC-specific JAG1 in adults led to reduced expression of myosin light-chain kinase and an impairment in the arterial contractile function [67].

3.4. Evaluation of Notch Signaling

For cellular experiments to quantify Notch signaling, the human embryonic kidney cell line HEK293 and mouse fibroblast cell line NIH 3T3 are often used because of their low-level expression of endogenous NOTCH receptors. A ligand-binding assay can be performed by adding a soluble ligand-Fc fusion protein to a medium of cultured cells expressing the NOTCH receptor to be quantified by flow cytometry or visualized by immunostaining [58,68]. To evaluate ligand-induced Notch signaling activity, cells expressing the Notch receptor (and luciferase reporter, if necessary) should be exposed to an immobilized ligand [69] or co-cultured with ligand-expressing cells [68]. Notch signaling activity can be evaluated by quantification of transcripts of the target genes or by the Notch reporter system using the HES1 promoter-luciferase construct or tandem repeats of the RBPj κ (also called CSL: CBF-1, Suppressor of Hairless, LAG-1) binding site-luciferase construct [70].

4. Strategy to Clarify Pathological Mechanism of CADASIL

This review focuses on basic research to clarify the pathophysiology of CADASIL. The two major viewpoints of research are as follows: the NOTCH3 signaling process and protein accumulation or aggregation. Researchers have used various materials, including human materials, animal models, cell cultures, and peptides, in order to clarify the pathophysiology of CADASIL (Table 1).

Table 1. Materials and applications to clarify the pathophysiology of CADASIL.

Human materials: autopsied brain tissue or vessels, skin biopsy specimens
Histopathology, immunohistochemistry
Biochemistry, proteomics
Gene expression, transcriptome
Animal models: transgenic mice
Genetic approach to clarify pathophysiology
Temporal analysis of disease process
Histopathology, immunohistochemistry
Biochemistry, proteomics
Gene expression, transcriptome
Cell cultures: VSMCs ¹ , iPS cell-derived mural cells, cell lines (HEK293, NIH 3T3, etc.)
Analysis of Notch signaling activity
Recreation of pathology of CADASIL
Viability and proliferation
In vitro
Aggregation assay of N3ECDpeptides

¹ vascular smooth muscle cells.

4.1. Mouse Models of CADASIL

4.1.1. Transgenic Mice

A CADASIL-like phenotype is not replicated in either the overexpression or knockout of wild-type *NOTCH3* in mice [25]. To date, R90C [71], R169C [72], R182C [73], C428S [74], C455R [75], and R1031C [75] *Notch3* transgenic mice, which harbor the CADASIL-causing mutations p.Arg90Cys, p.Arg169Cys, p.Arg182Cys, p.Cys428Ser, p.Cys455Arg, and p.Arg1031Cys, respectively, have been reported [25,76,77] (Table 2). Among the six mutations, pArg90Cys, p.Arg169Cys, and p.Arg182Cys are relatively frequent, whereas p.Cys428Ser, p.455Arg, and p.Arg1031Cys are rare in CADASIL patients [44]. The R169C transgene is a rat P1-derived artificial chromosome (PAC) containing the *Notch3* gene locus [72,78], and the R182C transgene is a human bacterial artificial chromosome (BAC)

containing *NOTCH3* and flanking genes [73,79]. Therefore, expression profiles of the transgenes of R169C and R182C show endogenous patterns. Transgene constructs of other mice are *Notch3* cDNA driven by the VSMC-specific *SM22 α* promoter (Table 2).

These transgenic mice successfully showed N3ECD accumulation and/or GOM deposition. However, a pathological white matter lesion was seen in only one model, R169C (line 88) [72], and cerebrovascular dysfunctions were reported in two models, R90C and R169C [72,78,80] (Table 2). Lacunar infarction and neurological symptoms, such as motor deficit, have never been reproduced in transgenic mouse models [25].

R169C mice showed the highest expression level of the transgene relative to endogenous *Notch3*, at 400%, and exhibited the earliest progression of pathological change, N3ECD accumulation at 1–2 months, GOM deposition at 5 months, and impaired cerebrovascular autoregulation at 5 months [72] (Table 2). R182C (line 350) also showed a high expression level of the transgene, at 350%, phenotypes from the early stage, N3ECD accumulation at 6 weeks, and GOM deposition at 5–6 months but failed to show cerebrovascular dysfunction [79].

Table 2. *NOTCH3* knock-in or transgenic mice.

Mouse (Line)	Mutation (EGFr)	Transgene Expression ¹	Brain Pathology	Vascular Physiology
Knock-in				
<i>Notch3R170C/R170C</i> [78,81]	p.Arg169Cys (EGFr4)	not applicable	N3ECD accumulation at 4 months [78]; GOM deposition at 20 months [81]	Decreased passive diameter of isolated posterior cerebral arteries at 4 months [78]
Human <i>NOTCH3</i> cDNA driven by murine <i>SM22α</i> promoter				
<i>mN3+/+; TghN3</i> (WT) (line 46) [82]	Wild-type	73%	No N3ECD accumulation; no GOM deposition	ND ²
<i>mN3+/+; TghN3(R90C)</i> (line Ma) [71,80,82]	p.Arg90Cys (EGFr 2)	86%	N3ECD accumulation and GOM deposition at 12 months [82]	Decreased flow-induced dilatation and increased pressure-induced myogenic tone in tail caudal arteries at 10–11 months [80]
<i>mN3+/+; TghN3</i> (C428S) (line 10) [74]	p.Cys428Ser (EGFr 10)	150%	N3ECD accumulation and GOM deposition at 8 months [74]	ND
PAC ³ containing genomic locus of rat <i>Notch3</i> [72,78]				
<i>TgNotch3R169C</i> (line 88)	p.Arg169Cys (EGFr 4)	400%	N3ECD accumulation at 1–2 months; GOM deposition at 5 months; white matter lesion (numerous vacuoles and loss of compact myelin with disorganized fibers) at 18–20 months [72]	Reduction of resting CBF ⁴ in gray matter (at 11–12 months) and white matter (at 18–20 months) [72]. Impaired cerebrovascular autoregulation at 5 months and attenuated functional hyperemia at 5–6 months [72]. Decreased increment of distensibility and decreased passive diameter in isolated posterior cerebral arteries at 6 and 2 months, respectively [78]
<i>TgNotch3R169C</i> (line 92)		200%	N3ECD accumulation and GOM deposition [25]	ND
<i>TgNotch3WT</i> (line 129)	Wild-type	400%	No N3ECD accumulation: no GOM deposition up to 20 months [72]	No impairment of resting CBF, cerebrovascular autoregulation, or functional hyperemia [72].

Table 2. Cont.

Mouse (Line)	Mutation (EGFr)	Transgene Expression ¹	Brain Pathology	Vascular Physiology
BAC ⁵ containing genomic locus of human <i>NOTCH3</i> [73,79]				
<i>tgN3MUT</i> (line 350)		350%	N3ECD accumulation detected at 6 weeks: GOM deposition detected at 5–6 months [73]; no white matter lesion detected [73]	No functional deficit in CBF [79].
<i>tgN3MUT</i> (line 200)	p.Arg182Cys (EGFr 4)	200%	N3ECD accumulation detected at 3 months [73]	ND
<i>tgN3MUT</i> (line 150)		150%	N3ECD accumulation detected at 5 months [73]	ND
<i>tgN3MUT</i> (line 100)		100%	N3ECD accumulation detected at 12 months [73]	No functional deficit in CBF [79].
<i>tgN3WT</i>	Wild-type	100%	No N3ECD accumulation; no GOM deposition up to 20 months [73]	No functional deficit in CBF [79].
Human <i>NOTCH3</i> cDNA, <i>SM22-Cre</i> mediated conditional knock-in into <i>ROSA26</i> locus [75]				
<i>NOTCH3C455R</i>	p.Cys455Arg (EGFr 11)	ND	GOM deposition at 6 months [75]	ND
<i>NOTCH3R1031C</i>	p.Arg1031Cys (EGFr 26)	ND	GOM deposition at 12 months [75]	ND

¹ Expression level of transgene relative to endogenous *Notch3*. ² ND: not described ³ P1-derived artificial chromosome. ⁴ CBF: cerebral blood flow. ⁵ Bacterial artificial chromosome.

4.1.2. Knock-In Mice

Of the two *Notch3* knock-in mice reported, one carrying p.Arg142Cys, corresponding to p.Arg141Cys in human *NOTCH3*, failed to develop any phenotype related to CADASIL [83]. In contrast, the other carrying p.Arg170Cys, corresponding to p.Arg169Cys in human *NOTCH3*, showed both the pathological and clinical characteristics of CADASIL [81]. p.Arg170Cys knock-in mice displayed GOM deposits and cerebral small vessel pathology, including thrombosis, microbleeds, and microinfarction, and also neurological symptoms including ataxia and paresis [81]. The phenotype was not observed in all animals analyzed. Of the 73 knock-in mice, brain pathology and motor defects were observed in 17 (23%) and 9 (12%), respectively, suggesting incomplete penetrance [81].

4.2. Cellular Model of CADASIL

4.2.1. Human VSMC Cells

To investigate cellular function predisposing to CADASIL, rather than replicate the disease phenotype, some studies used partially immortalized VSMCs established from the umbilical cords of newborns whose mothers had CADASIL [69,84,85]. Jin et al. identified the gene encoding platelet-derived growth factor receptor β (PDGFR β), a key molecule for vascular development and homeostasis, as a novel Notch signaling target gene [69]. Panahi et al. reported an increased expression of the *tumor growth factor β* (*TGF β*) gene in association with a decreased proliferation rate of CADASIL VSMCs [85]. On the other hand, an increased growth rate was observed in a primary VSMC culture prepared from skin biopsy samples by Neves et al. [86]. The reason for this discrepancy remains unresolved.

4.2.2. iPSC-Derived Mural Cells

Recently, Yamamoto et al. developed mural cells (VSMCs and pericytes) derived from induced pluripotent stem cells (iPS cells) of patients as a cell model of CADASIL [87]. Using the cells, they successfully reproduced previously reported CADASIL-related patho-

logical findings. They identified increased intracellular immunoreactivity of N3ECD and N3ECD-positive deposits on the plasma membrane, in agreement with their previous findings in autopsied brains [28]. In addition, some deposits were positive for latent-transforming growth factor beta-binding protein-1 (LTBP-1) or high-temperature requirement A1 (HTRA1), which were reported as components of GOM [88,89] (see Section 6.2). The cells also showed an irregular distribution of actin filaments and increased immunoreactivity of PDGFR β , in agreement with previous reports [90,91].

4.3. In Vitro Aggregation Assay

To investigate the pro-aggregation property of mutant NOTCH3, a single particle assay involving scanning for intensely fluorescent targets (SIFT) was developed [34,92]. When overexpressed, full-length N3ECD tends to be incorrectly folded in cells and is barely secreted in media. To obtain the unfolded recombinant N3ECD peptide of a sufficient dose from culture media, the peptide should be as short as EGFr 1–5 [34]. De novo multimer formation in a mixture of green or red fluorescent peptides can be detected by SIFT visualization. Aggregation was observed in mutant EGFr 1–5 and a mix of mutant and wild-type EGFr 1–5 but not in wild-type EGFr 1–5 [34]. The pro-aggregation abilities of some cysteine-sparing mutations, p.Arg75Pro and p.Asp80Gly, were shown by this analysis, supporting their pathogenicity [92]. Recently, Lee et al. reported structural changes in the EGFr 1–3 peptide using a gel mobility shift assay. They found an upshifted band in all the cysteine-altering mutants studied. They focused on substitution at Arg75 and found that p.Arg75Pro, p.Arg75Cys, and p.Arg75Gly peptides were upshifted, whereas substitutions from Arg75 to 16 other amino acids were not [93].

4.4. *Drosophila Melanogaster* and CADASIL

4.4.1. *Drosophila Melanogaster* and Human Neurological Diseases

Two major categories of neurological disorders are neurodegenerative and cerebrovascular ones. *Drosophila melanogaster* models of human neurodegenerative diseases, including Alzheimer's disease, Parkinson's disease, repeat expansion diseases, and amyotrophic lateral sclerosis (ALS)/frontotemporal lobar degeneration (FTLD), have been established [94–96]. Using fly models, the high-throughput screening of modifier genes and candidate drugs is possible [97]. On the other hand, it is difficult to create *Drosophila* models of human cerebrovascular diseases, mainly because of differences in the circulatory system between insects and mammals [98]. Flies have an open circulatory system; that is, the body cavity is filled with hemolymph circulated by a contractile dorsal tube called the heart. Although a *Drosophila* model of human cardiac disease is available [99], that of vascular disease is challenging.

4.4.2. *Drosophila* Notch Alleles Mimicking CADASIL-Causing Mutations

As described above, cysteine-altering mutations in a certain EGFr of NOTCH3 lead to a single phenotype, CADASIL, in humans. Some *Drosophila Notch* mutations have the same characteristics, but their phenotypes are not uniform (Tables 3 and 4). Notch signaling activity includes lateral inhibition, inductive signaling, and asymmetric cell division [100]. In *Drosophila* wings, *Notch* loss-of-function alleles cause thicker wing veins and scalloping (notching) in the wing margin. In contrast, *Notch* gain-of-function alleles, *Abruptex*, cause abrupt (shortened) wing veins and large wings [101]. All *Abruptex* mutations localize in EGFr 24–29, called the *Abruptex* domain. Of the *Abruptex* alleles, homozygous lethal alleles, known as *lethal-Abruptex*, were cysteine-altering mutations. Fryxell et al. hypothesized that human CADASIL corresponds to fly *Abruptex* because, at that time, known cysteine-altering mutations localized in the *Abruptex* domain [102]. *Abruptex* was considered as gain of function because its wing phenotype was the opposite to that of loss of function [103]. However, the ectopic activity of *Abruptex* was suggested [104], and subsequent studies showed that *Abruptex* phenotypes can be explained by a mild increase in Notch signaling and may have inhibitory effects in some contexts [47].

To date, increasing numbers of cysteine-altering mutations have been reported in fly *Notch* lines [105,106]. Their wing phenotypes were not uniform, including notching, Abruptex, and wild-type (Table 3). It is of note that some CADASIL mutations were reported at the residues corresponding to fly *N* alleles with the Notching or wild-type phenotype but never in those with the Abruptex phenotype (Table 3), which is contradictory to the hypothesis of Fryxell et al.

Table 3. *Drosophila Notch* (*N*) EGFr cysteine-altering alleles and wing phenotype.

<i>N</i> Allele	Fly Mutation (EGFr)	Wing Phenotype	Residue Corresponding to Human NOTCH3 (EGFr)	CADASIL Mutations Reported at the Residue ¹
			FlyBase [105]	
<i>N</i> ^{nd-3}	p.Cys105Phe (EGFr 2)	Notching	p.Cys87 (EGFr 2)	p.Cys87Arg [44]/Tyr [44]/Phe [107]
<i>N</i> ^{Mcd5}	p.Cys739Tyr (EGFr 18)	Wild-type	p.Cys681 (EGFr 17)	not reported
<i>N</i> ^{Ax-59b}	p.Cys972Gly (EGFr 24)	Abruptex	p.Cys875 (EGFr 22)	not reported
<i>N</i> ^{Ax-M1}	p.Cys999Tyr (EGFr 25)	Abruptex	p.Cys901 (EGFr 23)	not reported
			Yamamoto et al., 2012 [106]	
egf8-C2S	p.Cys343Ser (EGFr 8)	Notching	p.Cys285 (EGFr 7)	p.Cys285Arg [108]
egf8-C2Y	p.Cys343Tyr (EGFr 8)	Notching	p.Cys285 (EGFr 7)	p.Cys285Arg [108]
egf8-C6S	p.Cys369Ser (EGFr 8)	Notching	p.Cys311 (EGFr 7)	p.Cys311Ser [109,110]/Gly [111]
egf9-C5Y	p.Cys398Tyr (EGFr 9)	Notching	p.Cys340 (EGFr 8)	p.Cys340Phe [8]/Trp [112]
egf9-C6S	p.Cys407Ser (EGFr 9)	Notching	p.Cys349 (EGFr 8)	not reported
egf10-C2S	p.Cys413Ser (EGFr 10)	Notching	p.Cys355 (EGFr 9)	p.Cys355Ser ² [113]
egf11-C1S	p.Cys453Ser (EGFr 11)	Notching	p.Cys395 (EGFr 10)	p.Cys395Arg [44]
egf13-C2S	p.Cys535Ser (EGFr 13)	Wild-type	p.Cys478 (EGFr 12)	p.Cys478Tyr [114]
egf25-C2S	p.Cys993Ser (EGFr 25)	Notching	p.Cys896 (EGFr 23)	not reported
egf29-C2S	p.Cys1155Ser (EGFr 29)	Abruptex	p.Cys1055 (EGFr 27)	not reported
egf34-C1Y	p.Cys1341Tyr (EGFr 34)	Wild-type	p.Cys1250 (EGFr 32)	p.Cys1250Trp [115]/Gly ² [113]

¹ CADASIL mutations were identified using HGMD Professional (2023.3) [54]. ² p.Cys355Ser and p.Cys1250Gly are described by genome position (GRCh38) 19:15189401_C/G and 19:15178912_A/C, respectively.

Using *Drosophila*, lateral inhibition, inductive signaling, asymmetric cell division, and intracellular Notch trafficking can be analyzed in vivo. Nurmahdi et al. focused on 19 Notch missense mutations, 9 of which were cysteine-altering mutations in EGFr [116]. As summarized in Table 4, defects of signaling and trafficking tend to be milder as the mutant EGFr locates to the C-terminal, in other words, increasing the numbering of EGFr. This is consistent with the EGFr location–phenotype correlation reported in CADASIL (see Section 2.5.4). Although all mutations showed a defect in bristle formation, some mutations showed an impaired effect, and others were normal regarding lateral inhibition and inductive signaling (Table 4). These diverse effects and wing phenotypes (Table 3) may be due to the location of mutation (EGFr) and/or context-dependent role of Notch signaling. However, whether each mutation reflects the pathophysiology of CADASIL remains unknown. To our knowledge, the accumulation of the NECD in extracellular spaces has not been reported in *Drosophila*. Thus, the possibility of GOM-like deposits and their association with Notch signaling in the fly remain unknown.

Taken together, it may be difficult to determine which allele of fly *Notch* corresponds to CADASIL. However, studies of *Drosophila* Notch may be helpful to clarify the function of CADASIL-causing mutations, because EGFr-specific function and interactions between EGFRs in vivo have been intensively studied in *Drosophila* [47].

Table 4. Notch signaling and intracellular trafficking in *Drosophila Notch (N)* EGFr cysteine-altering alleles.

N Allele	Mutation (EGFr)	Bristle Formation ¹	Lateral Inhibition ²	Inductive Signaling ³	Intracellular Trafficking (Localization)
N ^X	p.Cys343Ser (EGFr 8)	Absent	Neurogenic	Depletion	Abnormal (loss of expression)
N ^{Omicron}	p.Cys343Tyr (EGFr 8)	Absent	Neurogenic	Depletion	Abnormal (ER ⁴)
N ^{Gamma}	p.Cys398Tyr (EGFr 9)	Absent	Neurogenic	Depletion	Abnormal (ER)
N ^S	p.Cys407Ser (EGFr 9)	Absent	Neurogenic	Depletion	Abnormal (ER)
N ^{Iota}	p.Cys413Ser (EGFr 10)	Absent	Neurogenic	Depletion	Abnormal (ER)
N ^G	p.Cys535Ser (EGFr 13)	Absent	Brain deformation	Depletion	Normal
N ^{Zeta}	p.Cys993Ser (EGFr 25)	Absent	Neurogenic	Depletion	Abnormal (ER)
N ^H	p.Cys1155Ser (EGFr 29)	Absent	Normal	Normal	Abnormal (Early endosomes)
N ^J	p.Cys1341Tyr (EGFr 34)	Absent	Normal	Normal	Normal

Modified from Nurmahdi et al., 2022 [116]. ¹ Defects of bristle formation reflect defects in lateral inhibition and asymmetric cell division. ² Defects of lateral inhibition in the embryonic central nervous system are neurogenic. Brain deformation reflects region-specific impairment of lateral inhibition. ³ Inductive signaling was evaluated by boundary cell formation in the embryonic hindgut. ⁴ ER: endoplasmic reticulum.

5. Notch Signaling in CADASIL

5.1. Biological Role of NOTCH3 Signaling in Vessels

Following the identification of *NOTCH3* as a causative gene for CADASIL, not only the pathological but also the biological role of *NOTCH3* in vessels have been focused on. The primary targets of CADASIL are VSMCs of small arteries and pericytes of capillaries [13,24]. Immunohistochemical and in situ hybridization analysis showed that, in the post-developmental stage, *NOTCH3* is normally expressed in VSMCs in arteries and also pericytes in capillaries [24,26,117]. *Notch3* knockout mice were fertile, viable, and normally developed [118] but did not show a CADASIL-like phenotype including GOM [25,119,120]. However, detailed analysis revealed abnormal patterning of the cerebrovascular structure, impaired postnatal differentiation, and myogenic tone of VSMCs, suggesting roles of *Notch3* in postnatal vasculature differentiation and VSMC maturation [25,121]. Thinning and disorganization of the tunica media of the tail and cerebral arteries [122] and increased susceptibility to brain ischemia [123] were also reported. Transcriptome analysis identified *Notch3* target genes, robustly downregulated in distal arteries of *Notch3*-null mice [124]. In addition, temporal changes in α -smooth muscle cell actin (SMA) staining of the retinal artery in *Notch3* knockout mice until 20 postnatal days showed progressive loss of VSMCs, suggesting an important role of *Notch3* in VSMC survival [125]. Some patients with bi-allelic loss-of-function mutations of *NOTCH3* were reported [55–57]. The patients had some CADASIL-like features, including arteriopathy, leukoencephalopathy, and stroke, but they were distinct from CADASIL patients because of child onset, no GOM, and other characteristic features. One patient had a homozygous nonsense *NOTCH3* mutation, p.Cys966Ter, and was initially diagnosed with Sneddon syndrome [55]. The expression levels of some of the *NOTCH3* target genes identified in *Notch3*-null mice [124] were decreased in skeletal muscle tissues of the patient and, notably, also CADASIL patients [55], suggesting decreased *NOTCH3* signaling in CADASIL. Two patients from another family were similar to the first case in having a homozygous nonsense mutation, p.Arg735Ter, and Sneddon syndrome [56]. Other patients did not have Sneddon syndrome and had the homozygous frameshift mutation p.Arg10Hisfs*16 or compound heterozygous mutations, p.His1944Tyr and p.Leu1976Profs*11 [57]. p.His1944Tyr is located in ANK in NICD, considered as loss of function because His1944 is conserved in the ALHWAAAVNN motif across vertebrates [57].

Although *Notch3* knockout mice did not show GOM, their VSMC phenotype exhibited some similarities with CADASIL model mice and *NOTCH3*-related patients. In tail arteries of *Notch3* null mice, VSMCs showed an irregular shape and smaller size and did not reach their appropriate place and orientation, leading to a disorganized tunica media composed of non-cohesive VSMCs, accompanied by an enlargement of VSMC intercellular

spaces [121]. Retinal arteries in *Notch3* knockout mice showed a progressive loss of VSMCs and thickened basement membranes [125]. Immature tail arteries at birth were indistinguishable between *Notch3* knockout and wild-type mice, suggesting an impairment in the postnatal maturation of VSMCs in mice. These VSMC phenotypes, including a decreasing number of VSMCs, morphological change and disorientation of VSMCs, and enlargement of VSMC intercellular spaces and/or thickened basement membranes, appear to overlap with those in a patient with bi-allelic loss-of-function *NOTCH3* mutations [55], CADASIL patients [12,55], and *Notch3* R90C transgenic mice [71]. Taken together, the impairment of VSMC maturation or maintenance of the maturation state, at least partially, may contribute to the pathophysiology of CADASIL.

5.2. NOTCH3 Signaling Process in CADASIL Pathophysiology

5.2.1. NOTCH3 Signaling Activity in CADASIL

CADASIL-causing mutations localize in EGFr of N3ECD, indicating that N3ICD is intact in CADASIL patients. Most mutations localized outside of the ligand-binding domain EGFr 10–11 and showed normal ligand binding and Notch signaling activity in cellular experiments [33,53,68,126]. On the other hand, relatively rare mutations in the ligand-binding domain, including p.Cys428Ser in EGFr 10 [53] and p.Cys455Arg in EGFr 11 [126], showed decreased ligand binding and Notch signaling activities. Stroke susceptibility of *Notch3* knockout mice was rescued by VSMC-specific expression of the p.Arg1031Cys (R1031C) transgene but not rescued by the p.Cys455Arg (C455R) transgene, indicating decreased Notch signaling of p.Cys455Arg in vivo [75]. Recently, Hack et al. investigated the NOTCH3 signaling activity of mutant NOTCH3 using NIH 3T3 cells. They reported lower signaling activity in mutations, both inside and outside of EGFr 10–11, compared with the wild-type [46].

In contrast to cellular experiments, Baron-Menguy et al. suggested increased Notch signaling in a mouse model of CADASIL. They noted a mild, 1.4–1.7-fold change but a significant increase in the expression of Notch3 target genes in TgNotch3R169C (line 88) compared with TgNotch3WT (line 92). In addition, the genetic reduction in Notch3 signaling by conditional specific knockdown of *Rbpj* in VSMC ameliorated the reduction in the passive diameter of cerebral arteries of TgNotch3R169C [78].

It is noteworthy that Kofler et al. reported the presence of GOM deposits in *Notch3*−/−; *Notch1*+/− double transgenic mice but not in *Notch3*−/− mice [127]. The secreted mutant N3ECD may bind to other vascular Notch family members, resulting in the blocking of their signaling. As both Notch1 and 3 are expressed in VSMCs, Notch1 may compensate for the dysfunction of mutant Notch3 in vivo. In *Notch3*−/−; *Notch1*+/− mice, a decreased dose of *Notch1* may be insufficient to compensate for total Notch signaling activity. Their finding that GOMs form in *Notch3*−/−; *Notch1*+/− can be interpreted as follows: very low total Notch signaling activity in VSMCs causes GOMs (in this case, Notch3-negative GOMs). Their finding suggests that N3ECD-positive GOMs in CADASIL may be a consequence of total Notch signaling dysfunction in VSMCs [127].

5.2.2. Transendocytosis of N3ECD

Previous pathological studies detected GOM in most mutations, including signal-defecting ones, p.Cys428Ser [21,74], and p.Cys455Arg [75]. This suggests that mutant N3ECD accumulates and leads to GOM deposits, regardless of signaling activity. However, the mechanism of the extracellular accumulation of mutant N3ECD remains unknown. By coculturing a stable *NOTCH3*-HEK293 cell line and *JAG1*-HEK293 cell line, Watanebe-Hosomi et al. noted a delayed degradation of p.Cys185Arg mutant N3ECD compared with the wild-type on the cell surface and hypothesized the impairment of transendocytosis in mutant N3ECD [128]. Based on this hypothesis, mutant N3ECD with attenuated ligand-binding activity is considered to accumulate more slowly than N3ECD with common mutations. This is in agreement with the finding that patients with EGFr 10–11 mutations were associated with a relatively preserved cognitive function

compared with those with common mutations [74]. In contrast, by coculturing stable *NOTCH3*-HEK293 and *JAG1*-NIH 3T3 cell lines, Suzuki et al. reported that transendocytosis was intact in p.Cys185Arg, whereas it was fully impaired in p.Cys428Ser [129]. They concluded that the accumulation of p.Cys185Arg may not be related to transendocytosis and that the accumulation of p.Cys428Ser N3ECD may be due to impaired transendocytosis. The reason for these contradictory findings remains unclear, but it may be partly due to differences in experimental conditions.

5.2.3. Cis-Interaction

Cis-interaction must be addressed, because both *NOTCH3* and its ligand *JAG1* are expressed in VSMCs. Cis-interaction is commonly known to inhibit Notch signaling through cis-inhibition of Notch by its ligand or cis-inhibition of its ligand by Notch [130]. Recent studies also reported the possibility of cis-activation [131,132]. Aberrant Notch signaling activities of *NOTCH3* mutations, previously reported (see Section 5.2.1), might be at least partially due to impaired cis-interaction. However, to our knowledge, the involvement of cis-interaction between *NOTCH3* and *JAG1* in CADASIL pathophysiology has not been reported to date.

5.2.4. Glycosylation of N3ECD

Studies focusing on the post-translational processing of CADASIL-causing mutations are limited. Arboleda-Velasquez focused on glycosylation and reported that the CADASIL-causing mutation impaired Fringe-mediated *O*-fucose elongation on *NOTCH3* using CHO Lec 1 cells co-transfected with *NOTCH3* EGFr 1–5 and *Fringe* [133]. Suzuki et al. reported that the lunatic fringe may increase the aggregation propensity of mutant *NOTCH3* using HeLa cells co-transfected with full-length *NOTCH3* and *lunatic fringe* [129].

6. Protein Accumulation or Aggregation in CADASIL

6.1. *TIMP3* and *VTN*

Monet-Lepretre et al. performed proteomic analysis of an N3ECD-enriched fraction prepared from frozen brain tissues of one CADASIL patient and one control individual, and they identified 104 proteins enriched in CADASIL [134]. Of the 104 proteins, they focused on Metalloproteinase inhibitor 3 (*TIMP3*) and Vitronectin (*VTN*), both of which are functionally important extracellular matrix (ECM) proteins. *TIMP3* and *VTN* were also present in brain artery samples of *NOTCH3* R90C transgenic mice but absent in *NOTCH3* wild-type transgenic mice [134]. Immunohistochemical analysis of the CADASIL brain confirmed the co-localization of *TIMP3* and *VTN* with N3ECD-positive aggregates. Through electron microscopic analysis, they successfully detected *TIMP3* immunogold labeling in GOM, whereas a suitable antibody was not available for *VTN*. Through further cellular experiments and an immunoprecipitation assay, they showed that the aggregation of N3ECD enhanced N3ECD-*TIMP3* complex formation, and *TIMP3* promoted complex formation including N3ECD and *VTN*. These observations support the N3ECD cascade hypothesis that N3ECD accumulation initiates GOM formation by recruiting ECM proteins such as *TIMP3*, which recruits additional proteins such as *VTN* [3]. In other words, mutant N3ECD is considered to accumulate first, followed by *TIMP3* and *VTN*, in this order. The results of analysis of the genetic reduction in *TIMP3* or *VTN* in *TgNotch3*^{R169C} by Capone et al. were compatible with this hypothesis [135]. In *TgNotch3*^{R169C} mice, cerebral blood flow (CBF) deficit was detected at 5–6 months, much earlier than pathological white matter lesions at 18–20 months (Table 2) [72,78]. The CBF deficits, including impaired CBF responses to neural activity (functional hyperemia) and impaired CBF autoregulation, were ameliorated by the genetic reduction in *Timp3* but not in *Vtn*. In contrast, as a late deficit, the number of pathological white matter lesions was decreased by the genetic reduction in *Vtn* but not in *Timp3*. In *TgNotch3*^{R169C} mice, N3ECD accumulation and GOM deposition were observed at approximately the same stage as the detection of a CBF deficit. It was notable that both the numbers of N3ECD deposits and GOM in *TgNotch3*^{R169C} were unaffected

by the genetic reduction in *Timp3* or *Vtn*, supporting the suggestion that N3ECD accumulation occurs upstream of GOM [135]. Transgenic mice with an increased expression of human *TIMP3* mimicked the impaired vascular function phenotype of CADASIL transgenic mice [135]. Taken together, these findings suggest that accumulations of TIMP3 and VTN have divergent influences on CADASIL: TIMP3 on CBF deficit in the early stage and VTN on pathological WML in the late stage [135].

6.2. *LTBP-1 and HTRA1*

Cerebral autosomal recessive arteriopathy with subcortical infarcts and leukoencephalopathy (CARASIL) is a hereditary cerebral small vessel disease caused by mutation of *high-temperature requirement A serine peptidase 1 (HTRA1)*, being extremely rare and identified mainly in East Asia [136]. Transforming growth factor- β (TGF- β) is a multifunctional cytokine, and its signaling plays important roles in vascular development and disease [137]. HTRA1 cleaves pro-TGF- β , and the cleaved pro-TGF- β is degraded by the endoplasmic reticulum-associated degradation system [138]. Therefore, loss-of-function mutation *HTRA1* results in the stimulation of TGF- β signaling, which is considered to be a key pathophysiological mechanism of CARASIL and *HTRA1*-related cerebral small vessel disease [139].

Kast et al. focused on ECM proteins related to the TGF- β pathway, and they found that latent TGF- β binding protein 1 (LTBP-1) was strongly colocalized with N3ECD via analyzing brain tissues of CADASIL patients by immunostaining. The co-aggregation properties of N3ECD and LTBP-1 were confirmed by in vitro assays [88]. They suggested a role of dysregulated TGF- β signaling in CADASIL, although whether the signaling is increased or decreased remains unknown.

Zellner et al. performed proteome analysis of brain vessels from autopsied samples of six CADASIL patients and six controls. They identified 95 proteins showing increased abundance in patients. They noted a marked increase in the HTRA1 content, at 4.7-fold, in the patient group. They also confirmed that HTRA1 colocalized with N3ECD deposits in the affected vessels. These findings suggest that HTRA1 is sequestered in abnormal aggregation, resulting in a loss of its protease activity, which is supported by an increase in HTRA1 substrates in the proteome of patients [89].

Klose et al. investigated the interaction of NOTCH3 and HTRA1 in CADASIL [140,141]. They showed that Jagged-1 is a substrate of HTRA1, and *HTRA1*-silencing in human umbilical artery smooth muscle cells (HUASMCs) resulted in an increase in *Jagged-1* expression, considered as NOTCH3 signaling activity. Their finding is in agreement with a previous report of increased NOTCH3 signaling in CADASIL by Baron-Menguy et al. (see Section 5.2.1) [78]. Clarifying the crosstalk between NOTCH3 and HTRA1, in other words, CADASIL and CARASIL, is an attractive issue that warrants further investigation.

7. Conclusions

Researchers have intensively examined the pathophysiology of CADASIL (Figure 5). The effects of mutant N3ECD on NOTCH3 signaling have been studied, but the results differ among reports, partly due to differences in assay conditions. The hypothesis of ECM protein accumulation following mutant N3ECD accumulation is the most commonly adopted; however, the process prior to N3ECD accumulation still remains unknown. In addition, this review cannot support the suggestion that N3ECD accumulation and GOM deposits are the sole cause of VSMC death or that increased break down of the endothelial barrier and leakage in CADASIL lead to the infarcts. To clarify these points, a more appropriate model of CADASIL is necessary.

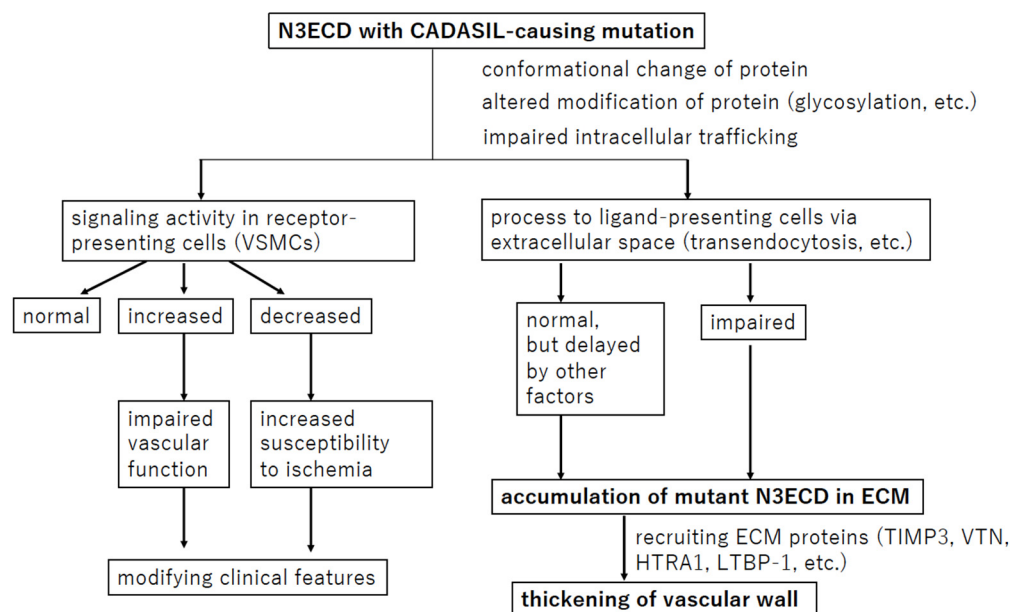


Figure 5. Overview of the hypothesis regarding the pathophysiology of CADASIL. The most widely held hypothesis and confirmed events are in bold.

Author Contributions: Writing—original draft preparation, I.M.; writing—review and editing, I.M., Y.N.-A., H.Y., M.Y. and T.M.; funding acquisition, I.M. and T.M. All authors have read and agreed to the published version of the manuscript.

Funding: This study was partially supported by JSPS KAKENHI Grant Number JP26461296 and JP21K07441 to I.M., a grant from SENSHIN Medical Research Foundation to T.M., the Grant for Joint Research Project of the Center for Advanced Insect Research Promotion, Kyoto Institute of Technology to I.M., the Japan Agency for Medical Research and Development (AMED, 17ek0109130s0703) to T.M., and by a grant-in-aid for Research on Intractable Disease (H28-Nanchitou(Nan)-Ippan-029, H30-Nanchitou(Nan)-Ippan-006, and 21FC1007) from the Japanese Ministry of Health, Labour, and Welfare, Japan to T.M.

Institutional Review Board Statement: Not applicable.

Informed Consent Statement: Not applicable.

Data Availability Statement: No new data were created or analyzed in this study. Data sharing is not applicable to this article.

Acknowledgments: We thank Shinya Yamamoto for helpful comments on this review. We also thank Justin Denley for English language editing.

Conflicts of Interest: M.Y. receives compensation from Kankyo Eisei Yakuhin Co., Ltd., a for-profit company that utilizes *Drosophila* for outsourcing services. The other authors declare no conflicts of interest.

References

- Chabriat, H.; Joutel, A.; Tournier-Lasserre, E.; Bousser, M.G. CADASIL: Yesterday, today, tomorrow. *Eur. J. Neurol.* **2020**, *27*, 1588–1595. [[CrossRef](#)]
- Chabriat, H.; Joutel, A.; Dichgans, M.; Tournier-Lasserre, E.; Bousser, M.G. Cadasil. *Lancet Neurol.* **2009**, *8*, 643–653. [[CrossRef](#)] [[PubMed](#)]
- Joutel, A. The NOTCH3^{ECD} cascade hypothesis of cerebral autosomal-dominant arteriopathy with subcortical infarcts and leukoencephalopathy disease. *Neurol. Clin. Neurosci.* **2015**, *3*, 1–6. [[CrossRef](#)]
- Caplan, L.R. Stroke: Etiology, classification, and epidemiology. In *UpToDate*; Kasner, S.E., Dashe, J.F., Eds.; Wolters Kluwer: Alphen aan den Rijn, The Netherlands, 2022.
- Rost, N.S. Definition, etiology, and clinical manifestations of transient ischemic attack. In *UpToDate*; Kasner, S.E., Dashe, J.F., Eds.; Wolters Kluwer: Alphen aan den Rijn, The Netherlands, 2022.

6. Pantoni, L. Cerebral small vessel disease: From pathogenesis and clinical characteristics to therapeutic challenges. *Lancet Neurol.* **2010**, *9*, 689–701. [[CrossRef](#)]
7. Dichgans, M.; Pulit, S.L.; Rosand, J. Stroke genetics: Discovery, biology, and clinical applications. *Lancet Neurol.* **2019**, *18*, 587–599. [[CrossRef](#)] [[PubMed](#)]
8. Rutten, J.W.; Dauwerse, H.G.; Gravesteijn, G.; van Belzen, M.J.; van der Grond, J.; Polke, J.M.; Bernal-Quiros, M.; Lesnik-Oberstein, S.A. Archetypal NOTCH3 mutations frequent in public exome: Implications for CADASIL. *Ann. Clin. Transl. Neurol.* **2016**, *3*, 844–853. [[CrossRef](#)] [[PubMed](#)]
9. Tournier-Lasserre, E.; Joutel, A.; Melki, J.; Weissenbach, J.; Lathrop, G.M.; Chabriat, H.; Mas, J.L.; Cabanis, E.A.; Baudrimont, M.; Maciazek, J.; et al. Cerebral autosomal dominant arteriopathy with subcortical infarcts and leukoencephalopathy maps to chromosome 19q12. *Nat. Genet.* **1993**, *3*, 256–259. [[CrossRef](#)]
10. Baudrimont, M.; Dubas, F.; Joutel, A.; Tournier-Lasserre, E.; Bousser, M.G. Autosomal dominant leukoencephalopathy and subcortical ischemic stroke. A clinicopathological study. *Stroke* **1993**, *24*, 122–125. [[CrossRef](#)]
11. Gutiérrez-Molina, M.; Caminero Rodríguez, A.; Martínez García, C.; Arpa Gutiérrez, J.; Morales Bastos, C.; Amer, G. Small arterial granular degeneration in familial Binswanger’s syndrome. *Acta Neuropathol.* **1994**, *87*, 98–105. [[CrossRef](#)]
12. Ruchoux, M.M.; Guerouaou, D.; Vandenhoute, B.; Pruvo, J.P.; Vermersch, P.; Leys, D. Systemic vascular smooth muscle cell impairment in cerebral autosomal dominant arteriopathy with subcortical infarcts and leukoencephalopathy. *Acta Neuropathol.* **1995**, *89*, 500–512.
13. Tikka, S.; Baumann, M.; Siitonen, M.; Pasanen, P.; Poyhonen, M.; Myllykangas, L.; Viitanen, M.; Fukutake, T.; Cognat, E.; Joutel, A.; et al. CADASIL and CARASIL. *Brain Pathol.* **2014**, *24*, 525–544. [[CrossRef](#)] [[PubMed](#)]
14. Wielaard, R.; Bornebroek, M.; Ophoff, R.A.; Winter-Warnars, H.A.; Scheltens, P.; Frants, R.R.; Ferrari, M.D.; Haan, J. A four-generation Dutch family with cerebral autosomal dominant arteriopathy with subcortical infarcts and leukoencephalopathy (CADASIL), linked to chromosome 19p13. *Clin. Neurol. Neurosurg.* **1995**, *97*, 307–313. [[CrossRef](#)] [[PubMed](#)]
15. Joutel, A.; Corpechot, C.; Ducros, A.; Vahedi, K.; Chabriat, H.; Mouton, P.; Alamowitch, S.; Domenga, V.; Cecillion, M.; Marechal, E.; et al. Notch3 mutations in CADASIL, a hereditary adult-onset condition causing stroke and dementia. *Nature* **1996**, *383*, 707–710. [[CrossRef](#)] [[PubMed](#)]
16. Mancuso, M.; Arnold, M.; Bersano, A.; Burlina, A.; Chabriat, H.; Debette, S.; Enzinger, C.; Federico, A.; Filla, A.; Finsterer, J.; et al. Monogenic cerebral small-vessel diseases: Diagnosis and therapy. Consensus recommendations of the European Academy of Neurology. *Eur. J. Neurol.* **2020**, *27*, 909–927. [[CrossRef](#)]
17. Mizuno, T. Diagnosis, pathomechanism and treatment of CADASIL. *Rinsho Shinkeigaku* **2012**, *52*, 303–313. [[CrossRef](#)]
18. Mizuno, T.; Muranishi, M.; Torugun, T.; Tango, H.; Nagakane, Y.; Kudeken, T.; Kawase, Y.; Kawabe, K.; Oshima, F.; Yaoi, T.; et al. Two Japanese CADASIL families exhibiting Notch3 mutation R75P not involving cysteine residue. *Intern. Med.* **2008**, *47*, 2067–2072.
19. Di Donato, I.; Bianchi, S.; De Stefano, N.; Dichgans, M.; Dotti, M.T.; Duering, M.; Jouvent, E.; Korczyn, A.D.; Lesnik-Oberstein, S.A.; Malandrini, A.; et al. Cerebral Autosomal Dominant Arteriopathy with Subcortical Infarcts and Leukoencephalopathy (CADASIL) as a model of small vessel disease: Update on clinical, diagnostic, and management aspects. *BMC Med.* **2017**, *15*, 41. [[CrossRef](#)]
20. Katan, M.; Luft, A. Global Burden of Stroke. *Semin. Neurol.* **2018**, *38*, 208–211. [[CrossRef](#)]
21. Buffon, F.; Porcher, R.; Hernandez, K.; Kurtz, A.; Pointeau, S.; Vahedi, K.; Bousser, M.G.; Chabriat, H. Cognitive profile in CADASIL. *J. Neurol. Neurosurg. Psychiatry* **2006**, *77*, 175–180. [[CrossRef](#)]
22. Lesnik-Oberstein, S.A.; van den Boom, R.; Middelkoop, H.A.; Ferrari, M.D.; Knaap, Y.M.; van Houwelingen, H.C.; Breuning, M.H.; van Buchem, M.A.; Haan, J. Incipient CADASIL. *Arch. Neurol.* **2003**, *60*, 707–712. [[CrossRef](#)]
23. Tikka, S.; Mykkanen, K.; Ruchoux, M.M.; Bergholm, R.; Junna, M.; Poyhonen, M.; Yki-Jarvinen, H.; Joutel, A.; Viitanen, M.; Baumann, M.; et al. Congruence between NOTCH3 mutations and GOM in 131 CADASIL patients. *Brain* **2009**, *132*, 933–939. [[CrossRef](#)] [[PubMed](#)]
24. Dziewulska, D.; Lewandowska, E. Pericytes as a new target for pathological processes in CADASIL. *Neuropathology* **2012**, *32*, 515–521. [[CrossRef](#)] [[PubMed](#)]
25. Joutel, A. Pathogenesis of CADASIL: Transgenic and knock-out mice to probe function and dysfunction of the mutated gene, Notch3, in the cerebrovasculature. *Bioessays* **2011**, *33*, 73–80. [[CrossRef](#)]
26. Joutel, A.; Andreux, F.; Gaulis, S.; Domenga, V.; Cecillon, M.; Battail, N.; Piga, N.; Chapon, F.; Godfrain, C.; Tournier-Lasserre, E. The ectodomain of the Notch3 receptor accumulates within the cerebrovasculature of CADASIL patients. *J. Clin. Investig.* **2000**, *105*, 597–605. [[CrossRef](#)] [[PubMed](#)]
27. Lorenzi, T.; Ragno, M.; Paolinelli, F.; Castellucci, C.; Scarpelli, M.; Morroni, M. CADASIL: Ultrastructural insights into the morphology of granular osmiophilic material. *Brain Behav.* **2017**, *7*, e00624. [[CrossRef](#)] [[PubMed](#)]
28. Yamamoto, Y.; Craggs, L.J.; Watanabe, A.; Booth, T.; Attems, J.; Low, R.W.; Oakley, A.E.; Kalaria, R.N. Brain microvascular accumulation and distribution of the NOTCH3 ectodomain and granular osmiophilic material in CADASIL. *J. Neuropathol. Exp. Neurol.* **2013**, *72*, 416–431. [[CrossRef](#)]
29. Ishiko, A.; Shimizu, A.; Nagata, E.; Takahashi, K.; Tabira, T.; Suzuki, N. Notch3 ectodomain is a major component of granular osmiophilic material (GOM) in CADASIL. *Acta Neuropathol.* **2006**, *112*, 333–339. [[CrossRef](#)] [[PubMed](#)]

30. Hack, R.; Rutten, J.; Lesnik Oberstein, S. CADASIL. In *GeneReviews*®; Adam, M.P., Feldman, J., Mirzaa, G.M., Pagon, R.A., Wallace, S.E., Bean, L.J.H., Gripp, K.W., Amemiya, A., Eds.; University of Washington: Seattle, WA, USA, 2000.
31. Rutten, J.W.; Haan, J.; Terwindt, G.M.; van Duinen, S.G.; Boon, E.M.; Lesnik Oberstein, S.A. Interpretation of *NOTCH3* mutations in the diagnosis of CADASIL. *Expert Rev. Mol. Diagn.* **2014**, *14*, 593–603. [[CrossRef](#)]
32. Mizuno, T.; Mizuta, I.; Watanabe-Hosomi, A.; Mukai, M.; Koizumi, T. Clinical and Genetic Aspects of CADASIL. *Front. Aging Neurosci.* **2020**, *12*, 91. [[CrossRef](#)]
33. Yamamoto, Y.; Liao, Y.C.; Lee, Y.C.; Ihara, M.; Choi, J.C. Update on the Epidemiology, Pathogenesis, and Biomarkers of Cerebral Autosomal Dominant Arteriopathy with Subcortical Infarcts and Leukoencephalopathy. *J. Clin. Neurol.* **2023**, *19*, 12–27. [[CrossRef](#)]
34. Duering, M.; Karpinska, A.; Rosner, S.; Hopfner, F.; Zechmeister, M.; Peters, N.; Kremmer, E.; Haffner, C.; Giese, A.; Dichgans, M.; et al. Co-aggregate formation of CADASIL-mutant *NOTCH3*: A single-particle analysis. *Hum. Mol. Genet.* **2011**, *20*, 3256–3265. [[CrossRef](#)] [[PubMed](#)]
35. Dichgans, M.; Ludwig, H.; Muller-Hocker, J.; Messerschmidt, A.; Gasser, T. Small in-frame deletions and missense mutations in CADASIL: 3D models predict misfolding of Notch3v EGF-like repeat domains. *Eur. J. Hum. Genet.* **2000**, *8*, 280–285. [[CrossRef](#)] [[PubMed](#)]
36. Muino, E.; Gallego-Fabrega, C.; Cullell, N.; Carrera, C.; Torres, N.; Krupinski, J.; Roquer, J.; Montaner, J.; Fernandez-Cadenas, I. Systematic Review of Cysteine-Sparing *NOTCH3* Missense Mutations in Patients with Clinical Suspicion of CADASIL. *Int. J. Mol. Sci.* **2017**, *18*, 1964. [[CrossRef](#)] [[PubMed](#)]
37. Kim, Y.E.; Yoon, C.W.; Seo, S.W.; Ki, C.S.; Kim, Y.B.; Kim, J.W.; Bang, O.Y.; Lee, K.H.; Kim, G.M.; Chung, C.S.; et al. Spectrum of *NOTCH3* mutations in Korean patients with clinically suspicious cerebral autosomal dominant arteriopathy with subcortical infarcts and leukoencephalopathy. *Neurobiol. Aging.* **2014**, *35*, 726.e1–726.e6. [[CrossRef](#)] [[PubMed](#)]
38. Ueda, A.; Ueda, M.; Nagatoshi, A.; Hirano, T.; Ito, T.; Arai, N.; Uyama, E.; Mori, K.; Nakamura, M.; Shinriki, S.; et al. Genotypic and phenotypic spectrum of CADASIL in Japan: The experience at a referral center in Kumamoto University from 1997 to 2014. *J. Neurol.* **2015**, *262*, 1828–1836. [[CrossRef](#)] [[PubMed](#)]
39. Mukai, M.; Mizuta, I.; Watanabe-Hosomi, A.; Koizumi, T.; Matsuura, J.; Hamano, A.; Tomimoto, H.; Mizuno, T. Genotype-phenotype correlations and effect of mutation location in Japanese CADASIL patients. *J. Hum. Genet.* **2020**, *65*, 637–646. [[CrossRef](#)]
40. Kim, Y.; Choi, E.J.; Choi, C.G.; Kim, G.; Choi, J.H.; Yoo, H.W.; Kim, J.S. Characteristics of CADASIL in Korea: A novel cysteine-sparing Notch3 mutation. *Neurology* **2006**, *66*, 1511–1516. [[CrossRef](#)]
41. Mukai, M.; Mizuta, I.; Ueda, A.; Nakashima, D.; Kushimura, Y.; Noto, Y.I.; Ohara, T.; Itoh, K.; Ando, Y.; Mizuno, T. A Japanese CADASIL patient with homozygous *NOTCH3* p.Arg544Cys mutation confirmed pathologically. *J. Neurol. Sci.* **2018**, *394*, 38–40. [[CrossRef](#)]
42. Choi, J.C.; Song, S.K.; Lee, J.S.; Kang, S.Y.; Kang, J.H. Diversity of stroke presentation in CADASIL: Study from patients harboring the predominant *NOTCH3* mutation R544C. *J. Stroke Cerebrovasc. Dis.* **2013**, *22*, 126–131. [[CrossRef](#)]
43. Liao, Y.C.; Hsiao, C.T.; Fuh, J.L.; Chern, C.M.; Lee, W.J.; Guo, Y.C.; Wang, S.J.; Lee, I.H.; Liu, Y.T.; Wang, Y.F.; et al. Characterization of CADASIL among the Han Chinese in Taiwan: Distinct Genotypic and Phenotypic Profiles. *PLoS ONE* **2015**, *10*, e0136501. [[CrossRef](#)]
44. Opherck, C.; Peters, N.; Herzog, J.; Luedtke, R.; Dichgans, M. Long-term prognosis and causes of death in CADASIL: A retrospective study in 411 patients. *Brain* **2004**, *127*, 2533–2539. [[CrossRef](#)]
45. Rutten, J.W.; Van Eijsden, B.J.; Duering, M.; Jouvent, E.; Opherck, C.; Pantoni, L.; Federico, A.; Dichgans, M.; Markus, H.S.; Chabriat, H.; et al. The effect of *NOTCH3* pathogenic variant position on CADASIL disease severity: *NOTCH3* EGFr 1–6 pathogenic variant are associated with a more severe phenotype and lower survival compared with EGFr 7–34 pathogenic variant. *Genet. Med.* **2019**, *21*, 676–682. [[CrossRef](#)]
46. Hack, R.J.; Gravesteijn, G.; Cerfontaine, M.N.; Santcroos, M.A.; Gatti, L.; Kopczak, A.; Bersano, A.; Duering, M.; Rutten, J.W.; Lesnik Oberstein, S.A.J. Three-tiered EGFr domain risk stratification for individualized *NOTCH3*-small vessel disease prediction. *Brain* **2023**, *146*, 2913–2927. [[CrossRef](#)] [[PubMed](#)]
47. Yamamoto, S. Making sense out of missense mutations: Mechanistic dissection of Notch receptors through structure-function studies in *Drosophila*. *Dev. Growth Differ.* **2020**, *62*, 15–34. [[CrossRef](#)] [[PubMed](#)]
48. Kopan, R.; Ilagan, M.X. The canonical Notch signaling pathway: Unfolding the activation mechanism. *Cell* **2009**, *137*, 216–233. [[CrossRef](#)] [[PubMed](#)]
49. Low, W.C.; Santa, Y.; Takahashi, K.; Tabira, T.; Kalaria, R.N. CADASIL-causing mutations do not alter Notch3 receptor processing and activation. *Neuroreport* **2006**, *17*, 945–949. [[CrossRef](#)]
50. Wang, T.; Baron, M.; Trump, D. An overview of Notch3 function in vascular smooth muscle cells. *Prog. Biophys. Mol. Biol.* **2008**, *96*, 499–509. [[CrossRef](#)]
51. Rebay, I.; Fleming, R.J.; Fehon, R.G.; Cherbas, L.; Cherbas, P.; Artavanis-Tsakonas, S. Specific EGF repeats of Notch mediate interactions with Delta and Serrate: Implications for Notch as a multifunctional receptor. *Cell* **1991**, *67*, 687–699. [[CrossRef](#)]
52. Arboleda-Velasquez, J.F.; Lopera, F.; Lopez, E.; Frosch, M.P.; Sepulveda-Falla, D.; Gutierrez, J.E.; Vargas, S.; Medina, M.; Martinez De Arrieta, C.; Lebo, R.V.; et al. C455R *notch3* mutation in a Colombian CADASIL kindred with early onset of stroke. *Neurology* **2002**, *59*, 277–279. [[CrossRef](#)]

53. Joutel, A.; Monet, M.; Domenga, V.; Riant, F.; Tournier-Lasserre, E. Pathogenic mutations associated with cerebral autosomal dominant arteriopathy with subcortical infarcts and leukoencephalopathy differently affect Jagged1 binding and Notch3 activity via the RBP/JK signaling Pathway. *Am. J. Hum. Genet.* **2004**, *74*, 338–347. [[CrossRef](#)]
54. Stenson, P.D.; Mort, M.; Ball, E.V.; Chapman, M.; Evans, K.; Azevedo, L.; Hayden, M.; Heywood, S.; Millar, D.S.; Phillips, A.D.; et al. The Human Gene Mutation Database (HGMD((R))): Optimizing its use in a clinical diagnostic or research setting. *Hum. Genet.* **2020**, *139*, 1197–1207. [[CrossRef](#)] [[PubMed](#)]
55. Pippucci, T.; Maresca, A.; Magini, P.; Cenacchi, G.; Donadio, V.; Palombo, F.; Papa, V.; Incensi, A.; Gasparre, G.; Valentino, M.L.; et al. Homozygous NOTCH3 null mutation and impaired NOTCH3 signaling in recessive early-onset arteriopathy and cavitating leukoencephalopathy. *EMBO Mol. Med.* **2015**, *7*, 848–858. [[CrossRef](#)] [[PubMed](#)]
56. Greisenegger, E.K.; Llufrui, S.; Chamorro, A.; Cervera, A.; Jimenez-Escrig, A.; Rappersberger, K.; Marik, W.; Greisenegger, S.; Stogmann, E.; Kopp, T.; et al. A NOTCH3 homozygous nonsense mutation in familial Sneddon syndrome with pediatric stroke. *J. Neurol.* **2021**, *268*, 810–816. [[CrossRef](#)] [[PubMed](#)]
57. Stellingwerff, M.D.; Nulton, C.; Helman, G.; Roosendaal, S.D.; Benko, W.S.; Pizzino, A.; Bugiani, M.; Vanderver, A.; Simons, C.; van der Knaap, M.S. Early-Onset Vascular Leukoencephalopathy Caused by Bi-Allelic NOTCH3 Variants. *Neuropediatrics* **2022**, *53*, 115–121. [[CrossRef](#)] [[PubMed](#)]
58. Nichols, J.T.; Miyamoto, A.; Olsen, S.L.; D’Souza, B.; Yao, C.; Weinmaster, G. DSL ligand endocytosis physically dissociates Notch1 heterodimers before activating proteolysis can occur. *J. Cell Biol.* **2007**, *176*, 445–458. [[CrossRef](#)]
59. van Tetering, G.; Vooijs, M. Proteolytic cleavage of Notch: “HIT and RUN”. *Curr. Mol. Med.* **2011**, *11*, 255–269. [[CrossRef](#)]
60. Prakash, N.; Hansson, E.; Betsholtz, C.; Mitsiadis, T.; Lendahl, U. Mouse Notch 3 expression in the pre- and postnatal brain: Relationship to the stroke and dementia syndrome CADASIL. *Exp. Cell Res.* **2002**, *278*, 31–44. [[CrossRef](#)]
61. Hofmann, J.J.; Luisa Iruela-Arispe, M. Notch expression patterns in the retina: An eye on receptor–ligand distribution during angiogenesis. *Gene Expr. Patterns* **2007**, *7*, 461–470. [[CrossRef](#)]
62. Hofmann, J.J.; Iruela-Arispe, M.L. Notch signaling in blood vessels: Who is talking to whom about what? *Circ. Res.* **2007**, *100*, 1556–1568. [[CrossRef](#)]
63. O’Hare, M.; Arboleda-Velasquez, J.F. Notch Signaling in Vascular Endothelial and Mural Cell Communications. *Cold Spring Harb. Perspect. Med.* **2022**, *12*, a041159. [[CrossRef](#)]
64. High, F.A.; Lu, M.M.; Pear, W.S.; Loomes, K.M.; Kaestner, K.H.; Epstein, J.A. Endothelial expression of the Notch ligand Jagged1 is required for vascular smooth muscle development. *Proc. Natl. Acad. Sci. USA* **2008**, *105*, 1955–1959. [[CrossRef](#)] [[PubMed](#)]
65. Breikaa, R.M.; Denman, K.; Ueyama, Y.; McCallinhardt, P.E.; Khan, A.Q.; Agarwal, G.; Trask, A.J.; Garg, V.; Lilly, B. Loss of Jagged1 in mature endothelial cells causes vascular dysfunction with alterations in smooth muscle phenotypes. *Vasc. Pharmacol.* **2022**, *145*, 107087. [[CrossRef](#)] [[PubMed](#)]
66. Feng, X.; Krebs, L.T.; Gridley, T. Patent ductus arteriosus in mice with smooth muscle-specific Jag1 deletion. *Development* **2010**, *137*, 4191–4199. [[CrossRef](#)] [[PubMed](#)]
67. Basu, S.; Barbur, I.; Calderon, A.; Banerjee, S.; Proweller, A. Notch signaling regulates arterial vasoreactivity through opposing functions of Jagged1 and Dll4 in the vessel wall. *Am. J. Physiol. Heart Circ. Physiol.* **2018**, *315*, H1835–H1850. [[CrossRef](#)] [[PubMed](#)]
68. Haritunians, T.; Chow, T.; De Lange, R.P.; Nichols, J.T.; Ghavimi, D.; Dorrani, N.; St Clair, D.M.; Weinmaster, G.; Schanen, C. Functional analysis of a recurrent missense mutation in Notch3 in CADASIL. *J. Neurol. Neurosurg. Psychiatry* **2005**, *76*, 1242–1248. [[CrossRef](#)] [[PubMed](#)]
69. Jin, S.; Hansson, E.M.; Tikka, S.; Lanner, F.; Sahlgren, C.; Farnebo, F.; Baumann, M.; Kalimo, H.; Lendahl, U. Notch signaling regulates platelet-derived growth factor receptor-beta expression in vascular smooth muscle cells. *Circ. Res.* **2008**, *102*, 1483–1491. [[CrossRef](#)] [[PubMed](#)]
70. Stockhausen, M.T.; Sjolund, J.; Axelson, H. Regulation of the Notch target gene Hes-1 by TGFalpha induced Ras/MAPK signaling in human neuroblastoma cells. *Exp. Cell Res.* **2005**, *310*, 218–228. [[CrossRef](#)]
71. Ruchoux, M.M.; Domenga, V.; Brulin, P.; Maciazek, J.; Limol, S.; Tournier-Lasserre, E.; Joutel, A. Transgenic Mice Expressing Mutant Notch3 Develop Vascular Alterations Characteristic of Cerebral Autosomal Dominant Arteriopathy with Subcortical Infarcts and Leukoencephalopathy. *Am. J. Pathol.* **2003**, *162*, 329–342. [[CrossRef](#)]
72. Joutel, A.; Monet-Lepretre, M.; Gosele, C.; Baron-Menguy, C.; Hammes, A.; Schmidt, S.; Lemaire-Carrette, B.; Domenga, V.; Schedl, A.; Lacombe, P.; et al. Cerebrovascular dysfunction and microcirculation rarefaction precede white matter lesions in a mouse genetic model of cerebral ischemic small vessel disease. *J. Clin. Investig.* **2010**, *120*, 433–445. [[CrossRef](#)]
73. Rutten, J.W.; Klever, R.R.; Hegeman, I.M.; Poole, D.S.; Dauwerse, H.G.; Broos, L.A.; Breukel, C.; Aartsma-Rus, A.M.; Verbeek, J.S.; van der Weerd, L.; et al. The NOTCH3 score: A pre-clinical CADASIL biomarker in a novel human genomic NOTCH3 transgenic mouse model with early progressive vascular NOTCH3 accumulation. *Acta Neuropathol. Commun.* **2015**, *3*, 89. [[CrossRef](#)]
74. Monet-Lepretre, M.; Bardot, B.; Lemaire, B.; Domenga, V.; Godin, O.; Dichgans, M.; Tournier-Lasserre, E.; Cohen-Tannoudji, M.; Chabriat, H.; Joutel, A. Distinct phenotypic and functional features of CADASIL mutations in the Notch3 ligand binding domain. *Brain* **2009**, *132*, 1601–1612. [[CrossRef](#)]
75. Arboleda-Velasquez, J.F.; Manent, J.; Lee, J.H.; Tikka, S.; Ospina, C.; Vanderburg, C.R.; Frosch, M.P.; Rodriguez-Falcon, M.; Villen, J.; Gygi, S.; et al. Hypomorphic Notch 3 alleles link Notch signaling to ischemic cerebral small-vessel disease. *Proc. Natl. Acad. Sci. USA* **2011**, *108*, E128–E135. [[CrossRef](#)] [[PubMed](#)]

76. Lee, J.H.; Bacskai, B.J.; Ayata, C. Genetic animal models of cerebral vasculopathies. *Prog. Mol. Biol. Transl. Sci.* **2012**, *105*, 25–55. [[CrossRef](#)]
77. Ayata, C. CADASIL: Experimental insights from animal models. *Stroke* **2010**, *41*, S129–S134. [[CrossRef](#)]
78. Baron-Menguy, C.; Domenga-Denier, V.; Ghezali, L.; Faraci, F.M.; Joutel, A. Increased Notch3 Activity Mediates Pathological Changes in Structure of Cerebral Arteries. *Hypertension* **2017**, *69*, 60–70. [[CrossRef](#)] [[PubMed](#)]
79. Gravesteyn, G.; Munting, L.P.; Overzier, M.; Mulder, A.A.; Hegeman, I.; Derieppe, M.; Koster, A.J.; van Duinen, S.G.; Meijer, O.C.; Aartsma-Rus, A.; et al. Progression and Classification of Granular Osmiophilic Material (GOM) Deposits in Functionally Characterized Human *NOTCH3* Transgenic Mice. *Transl. Stroke Res.* **2020**, *11*, 517–527. [[CrossRef](#)] [[PubMed](#)]
80. Dubroca, C.; Lacombe, P.; Domenga, V.; Maciazek, J.; Levy, B.; Tournier-Lasserre, E.; Joutel, A.; Henrion, D. Impaired vascular mechanotransduction in a transgenic mouse model of CADASIL arteriopathy. *Stroke* **2005**, *36*, 113–117. [[CrossRef](#)] [[PubMed](#)]
81. Wallays, G.; Nuyens, D.; Silasi-Mansat, R.; Souffreau, J.; Callaerts-Vegh, Z.; Van Nuffelen, A.; Moons, L.; D’Hooge, R.; Lupu, F.; Carmeliet, P.; et al. Notch3 Arg170Cys knock-in mice display pathologic and clinical features of the neurovascular disorder cerebral autosomal dominant arteriopathy with subcortical infarcts and leukoencephalopathy. *Arterioscler. Thromb. Vasc. Biol.* **2011**, *31*, 2881–2888. [[CrossRef](#)]
82. Monet, M.; Domenga, V.; Lemaire, B.; Souilhol, C.; Langa, F.; Babinet, C.; Gridley, T.; Tournier-Lasserre, E.; Cohen-Tannoudji, M.; Joutel, A. The archetypal R90C CADASIL-*NOTCH3* mutation retains NOTCH3 function in vivo. *Hum. Mol. Genet.* **2007**, *16*, 982–992. [[CrossRef](#)]
83. Lundkvist, J.; Zhu, S.; Hansson, E.M.; Schweinhardt, P.; Miao, Q.; Beatus, P.; Dannaeus, K.; Karlstrom, H.; Johansson, C.B.; Viitanen, M.; et al. Mice carrying a R142C Notch 3 knock-in mutation do not develop a CADASIL-like phenotype. *Genesis* **2005**, *41*, 13–22. [[CrossRef](#)]
84. Viitanen, M.; Sundstrom, E.; Baumann, M.; Poyhonen, M.; Tikka, S.; Behbahani, H. Experimental studies of mitochondrial function in CADASIL vascular smooth muscle cells. *Exp. Cell Res.* **2013**, *319*, 134–143. [[CrossRef](#)] [[PubMed](#)]
85. Panahi, M.; Yousefi Mesri, N.; Samuelsson, E.B.; Coupland, K.G.; Forsell, C.; Graff, C.; Tikka, S.; Winblad, B.; Viitanen, M.; Karlstrom, H.; et al. Differences in proliferation rate between CADASIL and control vascular smooth muscle cells are related to increased TGFbeta expression. *J. Cell. Mol. Med.* **2018**, *22*, 3016–3024. [[CrossRef](#)] [[PubMed](#)]
86. Neves, K.B.; Harvey, A.P.; Moreton, F.; Montezano, A.C.; Rios, F.J.; Alves-Lopes, R.; Nguyen Dinh Cat, A.; Rocchiccioli, P.; Delles, C.; Joutel, A.; et al. ER stress and Rho kinase activation underlie the vasculopathy of CADASIL. *JCI Insight* **2019**, *4*, e131344. [[CrossRef](#)] [[PubMed](#)]
87. Yamamoto, Y.; Kojima, K.; Taura, D.; Sone, M.; Washida, K.; Egawa, N.; Kondo, T.; Minakawa, E.N.; Tsukita, K.; Enami, T.; et al. Human iPS cell-derived mural cells as an in vitro model of hereditary cerebral small vessel disease. *Mol. Brain* **2020**, *13*, 38. [[CrossRef](#)] [[PubMed](#)]
88. Kast, J.; Hanecker, P.; Beaufort, N.; Giese, A.; Joutel, A.; Dichgans, M.; Opherk, C.; Haffner, C. Sequestration of latent TGF-beta binding protein 1 into CADASIL-related Notch3-ECD deposits. *Acta Neuropathol. Commun.* **2014**, *2*, 96. [[CrossRef](#)] [[PubMed](#)]
89. Zellner, A.; Scharrer, E.; Arzberger, T.; Oka, C.; Domenga-Denier, V.; Joutel, A.; Lichtenthaler, S.F.; Muller, S.A.; Dichgans, M.; Haffner, C. CADASIL brain vessels show a HTRA1 loss-of-function profile. *Acta Neuropathol.* **2018**, *136*, 111–125. [[CrossRef](#)] [[PubMed](#)]
90. Craggs, L.J.; Fenwick, R.; Oakley, A.E.; Ihara, M.; Kalaria, R.N. Immunolocalization of platelet-derived growth factor receptor-beta (PDGFR-beta) and pericytes in cerebral autosomal dominant arteriopathy with subcortical infarcts and leukoencephalopathy (CADASIL). *Neuropathol. Appl. Neurobiol.* **2015**, *41*, 557–570. [[CrossRef](#)] [[PubMed](#)]
91. Tikka, S.; Ng, Y.P.; Di Maio, G.; Mykkanen, K.; Siitonen, M.; Lepikhova, T.; Poyhonen, M.; Viitanen, M.; Virtanen, I.; Kalimo, H.; et al. CADASIL mutations and shRNA silencing of *NOTCH3* affect actin organization in cultured vascular smooth muscle cells. *J. Cereb. Blood Flow Metab.* **2012**, *32*, 2171–2180. [[CrossRef](#)]
92. Wollenweber, F.A.; Hanecker, P.; Bayer-Karpinska, A.; Malik, R.; Bazner, H.; Moreton, F.; Muir, K.W.; Muller, S.; Giese, A.; Opherk, C.; et al. Cysteine-sparing CADASIL mutations in *NOTCH3* show proaggregatory properties in vitro. *Stroke* **2015**, *46*, 786–792. [[CrossRef](#)]
93. Lee, S.J.; Zhang, X.; Wu, E.; Sukpraphrute, R.; Sukpraphrute, C.; Ye, A.; Wang, M.M. Structural changes in NOTCH3 induced by CADASIL mutations: Role of cysteine and non-cysteine alterations. *J. Biol. Chem.* **2023**, *299*, 104838. [[CrossRef](#)]
94. McGurk, L.; Berson, A.; Bonini, N.M. *Drosophila* as an In Vivo Model for Human Neurodegenerative Disease. *Genetics* **2015**, *201*, 377–402. [[CrossRef](#)]
95. Yamaguchi, M. (Ed.) *Drosophila Models for Human Diseases*; Springer: Singapore, 2018; Volume 1076.
96. Bolus, H.; Crocker, K.; Boekhoff-Falk, G.; Chtarbanova, S. Modeling Neurodegenerative Disorders in *Drosophila melanogaster*. *Int. J. Mol. Sci.* **2020**, *21*, 3055. [[CrossRef](#)] [[PubMed](#)]
97. Lambrechts, R.; Faber, A.; Sibon, O. Modelling in miniature: Using *Drosophila melanogaster* to study human neurodegeneration. *Drug Discov. Today Dis. Models* **2017**, *25–26*, 3–10. [[CrossRef](#)]
98. Miller, A. The internal anatomy and histology of the imago of *Drosophila melanogaster*. In *Biology of Drosophila*; Demerec, M., Ed.; John Wiley & Sons: New York, NY, USA, 1950.
99. Wolf, M.J.; Amrein, H.; Izatt, J.A.; Choma, M.A.; Reedy, M.C.; Rockman, H.A. *Drosophila* as a model for the identification of genes causing adult human heart disease. *Proc. Natl. Acad. Sci. USA* **2006**, *103*, 1394–1399. [[CrossRef](#)] [[PubMed](#)]
100. Bray, S.J. Notch signalling: A simple pathway becomes complex. *Nat. Rev. Mol. Cell Biol.* **2006**, *7*, 678–689. [[CrossRef](#)]

101. de Celis, J.F.; García-Bellido, A. Roles of the Notch gene in *Drosophila* wing morphogenesis. *Mech. Dev.* **1994**, *46*, 109–122. [[CrossRef](#)] [[PubMed](#)]
102. Fryxell, K.J.; Soderlund, M.; Jordan, T.V. An animal model for the molecular genetics of CADASIL. (Cerebral autosomal dominant arteriopathy with subcortical infarcts and leukoencephalopathy). *Stroke* **2001**, *32*, 6–11. [[CrossRef](#)]
103. de Celis, J.F.; Garcia-Bellido, A. Modifications of the notch function by *Abruptex* mutations in *Drosophila melanogaster*. *Genetics* **1994**, *136*, 183–194. [[CrossRef](#)]
104. Perez, L.; Milan, M.; Bray, S.; Cohen, S.M. Ligand-binding and signaling properties of the Ax[M1] form of Notch. *Mech. Dev.* **2005**, *122*, 479–486. [[CrossRef](#)]
105. FlyBase. Available online: <http://flybase.org> (accessed on 11 June 2020).
106. Yamamoto, S.; Charng, W.L.; Rana, N.A.; Kakuda, S.; Jaiswal, M.; Bayat, V.; Xiong, B.; Zhang, K.; Sandoval, H.; David, G.; et al. A mutation in EGF repeat-8 of Notch discriminates between Serrate/Jagged and Delta family ligands. *Science* **2012**, *338*, 1229–1232. [[CrossRef](#)]
107. Mizuta, I.; Watanabe-Hosomi, A.; Koizumi, T.; Mukai, M.; Hamano, A.; Tomii, Y.; Kondo, M.; Nakagawa, M.; Tomimoto, H.; Hirano, T.; et al. New diagnostic criteria for cerebral autosomal dominant arteriopathy with subcortical infarcts and leukoencephalopathy in Japan. *J. Neurol. Sci.* **2017**, *381*, 62–67. [[CrossRef](#)] [[PubMed](#)]
108. Okubo, M.; Doi, H.; Fukai, R.; Fujita, A.; Mitsuhashi, S.; Hashiguchi, S.; Kishida, H.; Ueda, N.; Morihara, K.; Ogasawara, A.; et al. GGC Repeat Expansion of NOTCH2NLC in Adult Patients with Leukoencephalopathy. *Ann. Neurol.* **2019**, *86*, 962–968. [[CrossRef](#)] [[PubMed](#)]
109. Moreton, F.C.; Razvi, S.S.; Davidson, R.; Muir, K.W. Changing clinical patterns and increasing prevalence in CADASIL. *Acta Neurol. Scand.* **2014**, *130*, 197–203. [[CrossRef](#)] [[PubMed](#)]
110. Gurung, A.; Bhattacharjee, S.; Nor, A.M. Headache in a middle-aged man due to a rare mutation in the NOTCH 3 gene. *Neurol. India* **2019**, *67*, 879–881. [[PubMed](#)]
111. Qi, Y.; Li, H.; Yu, L. Case report: Mild leukoencephalopathy caused by a new mutation of NOTCH3 gene. *Medicine* **2023**, *102*, e33289. [[CrossRef](#)]
112. Min, J.Y.; Park, S.J.; Kang, E.J.; Hwang, S.Y.; Han, S.H. Mutation spectrum and genotype-phenotype correlations in 157 Korean CADASIL patients: A multicenter study. *Neurogenetics* **2022**, *23*, 45–58. [[CrossRef](#)]
113. Cho, B.P.H.; Jolly, A.A.; Nannoni, S.; Tozer, D.; Bell, S.; Markus, H.S. Association of NOTCH3 Variant Position with Stroke Onset and Other Clinical Features among Patients with CADASIL. *Neurology* **2022**, *99*, e430–e439. [[CrossRef](#)]
114. Ozaki, K.; Irioka, T.; Ishikawa, K.; Mizusawa, H. CADASIL with a novel NOTCH3 mutation (Cys478Tyr). *J. Stroke Cerebrovasc. Dis.* **2015**, *24*, e61–e62. [[CrossRef](#)]
115. del Río-Espínola, A.; Fernández-Cadenas, I.; Mendióroz, M.; Gutiérrez-Agulló, M.; Fernández, M.T.; Fernández-Morales, J.; Maisterra, O.; Domingues-Montanari, S.; García-Patos, V.; Solé, E.; et al. Novel human pathological mutations. Gene symbol: NOTCH3. Disease: CADASIL. *Hum. Genet.* **2010**, *127*, 474.
116. Nurmahdi, H.; Hasegawa, M.; Mujizah, E.Y.; Sasamura, T.; Inaki, M.; Yamamoto, S.; Yamakawa, T.; Matsuno, K. Notch Missense Mutations in *Drosophila* Reveal Functions of Specific EGF-like Repeats in Notch Folding, Trafficking, and Signaling. *Biomolecules* **2022**, *12*, 1752. [[CrossRef](#)]
117. Winkler, E.A.; Bell, R.D.; Zlokovic, B.V. Central nervous system pericytes in health and disease. *Nat. Neurosci.* **2011**, *14*, 1398–1405. [[CrossRef](#)] [[PubMed](#)]
118. Krebs, L.T.; Xue, Y.; Norton, C.R.; Sundberg, J.P.; Beatus, P.; Lendahl, U.; Joutel, A.; Gridley, T. Characterization of *Notch3*-deficient mice: Normal embryonic development and absence of genetic interactions with a *Notch1* mutation. *Genesis* **2003**, *37*, 139–143. [[CrossRef](#)] [[PubMed](#)]
119. Kitamoto, T.; Takahashi, K.; Takimoto, H.; Tomizuka, K.; Hayasaka, M.; Tabira, T.; Hanaoka, K. Functional redundancy of the *Notch* gene family during mouse embryogenesis: Analysis of *Notch* gene expression in *Notch3*-deficient mice. *Biochem. Biophys. Res. Commun.* **2005**, *331*, 1154–1162. [[CrossRef](#)]
120. Manini, A.; Pantoni, L. CADASIL from Bench to Bedside: Disease Models and Novel Therapeutic Approaches. *Mol. Neurobiol.* **2021**, *58*, 2558–2573. [[CrossRef](#)] [[PubMed](#)]
121. Domenga, V.; Fardoux, P.; Lacombe, P.; Monet, M.; Maciazek, J.; Krebs, L.T.; Klonjowski, B.; Berrou, E.; Mericskay, M.; Li, Z.; et al. *Notch3* is required for arterial identity and maturation of vascular smooth muscle cells. *Genes Dev.* **2004**, *18*, 2730–2735. [[CrossRef](#)] [[PubMed](#)]
122. Belin de Chantemele, E.J.; Retailleau, K.; Pinaud, F.; Vessieres, E.; Bocquet, A.; Guihot, A.L.; Lemaire, B.; Domenga, V.; Baufreton, C.; Loufrani, L.; et al. Notch3 is a major regulator of vascular tone in cerebral and tail resistance arteries. *Arterioscler. Thromb. Vasc. Biol.* **2008**, *28*, 2216–2224. [[CrossRef](#)] [[PubMed](#)]
123. Arboleda-Velasquez, J.F.; Zhou, Z.; Shin, H.K.; Louvi, A.; Kim, H.H.; Savitz, S.I.; Liao, J.K.; Salomone, S.; Ayata, C.; Moskowitz, M.A.; et al. Linking Notch signaling to ischemic stroke. *Proc. Natl. Acad. Sci. USA* **2008**, *105*, 4856–4861. [[CrossRef](#)]
124. Fouillade, C.; Baron-Menguy, C.; Domenga-Denier, V.; Thibault, C.; Takamiya, K.; Haganir, R.; Joutel, A. Transcriptome analysis for Notch3 target genes identifies Grip2 as a novel regulator of myogenic response in the cerebrovasculature. *Arterioscler. Thromb. Vasc. Biol.* **2013**, *33*, 76–86. [[CrossRef](#)]

125. Henshall, T.L.; Keller, A.; He, L.; Johansson, B.R.; Wallgard, E.; Raschperger, E.; Mae, M.A.; Jin, S.; Betsholtz, C.; Lendahl, U. Notch3 is necessary for blood vessel integrity in the central nervous system. *Arterioscler. Thromb. Vasc. Biol.* **2015**, *35*, 409–420. [[CrossRef](#)]
126. Peters, N.; Opherk, C.; Zacherle, S.; Capell, A.; Gempel, P.; Dichgans, M. CADASIL-associated Notch3 mutations have differential effects both on ligand binding and ligand-induced Notch3 receptor signaling through RBP-Jk. *Exp. Cell Res.* **2004**, *299*, 454–464. [[CrossRef](#)]
127. Kofler, N.M.; Cuervo, H.; Uh, M.K.; Murtomaki, A.; Kitajewski, J. Combined deficiency of Notch1 and Notch3 causes pericyte dysfunction, models CADASIL, and results in arteriovenous malformations. *Sci. Rep.* **2015**, *5*, 16449. [[CrossRef](#)] [[PubMed](#)]
128. Watanabe-Hosomi, A.; Watanabe, Y.; Tanaka, M.; Nakagawa, M.; Mizuno, T. Transendocytosis is impaired in CADASIL-mutant NOTCH3. *Exp. Neurol.* **2012**, *233*, 303–311. [[CrossRef](#)] [[PubMed](#)]
129. Suzuki, S.; Hiura, S.; Mashiko, T.; Matsumoto, T.; Itoh, M. Lunatic fringe promotes the aggregation of CADASIL NOTCH3 mutant proteins. *Biochem. Biophys. Res. Commun.* **2021**, *557*, 302–308. [[CrossRef](#)] [[PubMed](#)]
130. del Alamo, D.; Rouault, H.; Schweisguth, F. Mechanism and significance of cis-inhibition in Notch signalling. *Curr. Biol.* **2011**, *21*, R40–R47. [[CrossRef](#)] [[PubMed](#)]
131. Nandagopal, N.; Santat, L.A.; Elowitz, M.B. Cis-activation in the Notch signaling pathway. *Elife* **2019**, *8*, e37880. [[CrossRef](#)] [[PubMed](#)]
132. Ng, H.L.; Quail, E.; Cruickshank, M.N.; Ulgiati, D. To Be, or Notch to Be: Mediating Cell Fate from Embryogenesis to Lymphopoiesis. *Biomolecules* **2021**, *11*, 849. [[CrossRef](#)] [[PubMed](#)]
133. Arboleda-Velasquez, J.F.; Rampal, R.; Fung, E.; Darland, D.C.; Liu, M.; Martinez, M.C.; Donahue, C.P.; Navarro-Gonzalez, M.F.; Libby, P.; D'Amore, P.A.; et al. CADASIL mutations impair Notch3 glycosylation by Fringe. *Hum. Mol. Genet.* **2005**, *14*, 1631–1639. [[CrossRef](#)]
134. Monet-Lepretre, M.; Haddad, I.; Baron-Menguy, C.; Fouillot-Panchal, M.; Riani, M.; Domenga-Denier, V.; Dussaule, C.; Cognat, E.; Vinh, J.; Joutel, A. Abnormal recruitment of extracellular matrix proteins by excess Notch3^{ECD}: A new pathomechanism in CADASIL. *Brain* **2013**, *136*, 1830–1845. [[CrossRef](#)]
135. Capone, C.; Cognat, E.; Ghezali, L.; Baron-Menguy, C.; Aubin, D.; Mesnard, L.; Stohr, H.; Domenga-Denier, V.; Nelson, M.T.; Joutel, A. Reducing Timp3 or vitronectin ameliorates disease manifestations in CADASIL mice. *Ann. Neurol.* **2016**, *79*, 387–403. [[CrossRef](#)]
136. Nozaki, H.; Nishizawa, M.; Onodera, O. Features of cerebral autosomal recessive arteriopathy with subcortical infarcts and leukoencephalopathy. *Stroke* **2014**, *45*, 3447–3453. [[CrossRef](#)]
137. ten Dijke, P.; Arthur, H.M. Extracellular control of TGFbeta signalling in vascular development and disease. *Nat. Rev. Mol. Cell Biol.* **2007**, *8*, 857–869. [[CrossRef](#)] [[PubMed](#)]
138. Shiga, A.; Nozaki, H.; Yokoseki, A.; Nihonmatsu, M.; Kawata, H.; Kato, T.; Koyama, A.; Arima, K.; Ikeda, M.; Katada, S.; et al. Cerebral small-vessel disease protein HTRA1 controls the amount of TGF-beta1 via cleavage of proTGF-beta1. *Hum. Mol. Genet.* **2011**, *20*, 1800–1810. [[CrossRef](#)] [[PubMed](#)]
139. Uemura, M.; Nozaki, H.; Kato, T.; Koyama, A.; Sakai, N.; Ando, S.; Kanazawa, M.; Hishikawa, N.; Nishimoto, Y.; Polavarapu, K.; et al. HTRA1-Related Cerebral Small Vessel Disease: A Review of the Literature. *Front. Neurol.* **2020**, *11*, 545. [[CrossRef](#)] [[PubMed](#)]
140. Klose, R.; Prinz, A.; Tetzlaff, F.; Weis, E.M.; Moll, I.; Rodriguez-Vita, J.; Oka, C.; Korff, T.; Fischer, A. Loss of the serine protease HTRA1 impairs smooth muscle cells maturation. *Sci. Rep.* **2019**, *9*, 18224. [[CrossRef](#)]
141. Klose, R.; Adam, M.G.; Weis, E.M.; Moll, I.; Wustehube-Lausch, J.; Tetzlaff, F.; Oka, C.; Ehrmann, M.; Fischer, A. Inactivation of the serine protease HTRA1 inhibits tumor growth by deregulating angiogenesis. *Oncogene* **2018**, *37*, 4260–4272. [[CrossRef](#)]

Disclaimer/Publisher's Note: The statements, opinions and data contained in all publications are solely those of the individual author(s) and contributor(s) and not of MDPI and/or the editor(s). MDPI and/or the editor(s) disclaim responsibility for any injury to people or property resulting from any ideas, methods, instructions or products referred to in the content.